Thomas-Fermi model for dense plasmas

Ruoxian Ying* and G. Kalman
Department of Physics, Boston College, Chestnut Hill, Massachusetts 02167
(Received 29 August 1988)

The average degree of ionization for a dense plasma is calculated with the aid of a newly established atomic model based on the Thomas-Fermi (TF) method. This new model is characterized by the following features: (i) the bound electrons and free electrons are treated separately, (ii) a physically reasonable definition of the bound electrons is given, (iii) the system is described as a strongly coupled plasma of free electrons and TF ions, (iv) the source density in the Poisson equation is determined by the electron-ion and ion-ion correlation functions, and (v) the degree of ionization is calculated through the minimization of the total free energy. Results from the first and second approximations are presented, corresponding to models of increasing sophistication for the ion-ion correlation function. A comparison of these results with the results from earlier TF calculations and with the results from the Saha equation is also provided.

I. INTRODUCTION

In two-component plasmas, electrons and ions can combine into other ions and atoms, i.e., bound states exist. On the other hand, atoms can become ionized into electrons and ions. The existence of these two opposite processes, the recombination and ionization, leads to the establishment of an equilibrium in which a certain fraction of the total number of particles (atoms and ions) are in various stages of ionization. The different ionization states can be characterized by the degree of ionization, which is defined as the ratio of the number of free electrons to the number of other particles (except electrons).

The degree of ionization has a strong effect on many plasma properties. An accurate calculation of the degree of ionization is required for quantitative modeling of plasma dynamics. In the dense plasma regime, the degree of ionization is an important characteristic in inertial confinement fusion and astrophysics. Knowledge of average ionization is needed, for example, in understanding the energy transport and deposition properties of fusion plasmas or the equation of state in stellar interior. The establishment of the precise equilibrium degree of ionization is a complex many-body process, determined by the competition between the bound states affected by the many-body interaction and the "free-particle" or scattering states where the many-body interaction plays a crucial role. In a plasma, the nature of the many-body interaction is characterized by the set of coupling parameters between species A and B, $\Gamma_{AB}=Z_A Z_B e^2/kTd_{AB}$ (d_{Ab} is the interparticle distance, $Z_A e$ is the species charge). The determination of the degree of ionization becomes especially difficult when the plasma is strongly coupled, i.e., when at least $\Gamma_{ii} \geq 1$.

A variety of different methods has been adopted to determine the degree of ionization for strongly coupled plasmas; the Saha-equation method[1-4] and Thomas-Fermi (TF) statistical atomic model[5-8] provide paradigms for the two distinct approaches into which the various approximation schemes can be classified. In the first, one considers a distribution of various ionization states z, $z=0,1,2,\ldots,Z$ (where Z is the nuclear charge) and determines the number of particles in each of them. In the second, one focuses on an "average atom" whose ionization is given by a generally fractional number z, $0 \leq z \leq Z$.

The main problem in the Saha-equation approach is how to determine the bound-state energies in the presence of the many-body environment and how to assure self-consistency. Work along these lines has been mainly restricted to using a Debye potential within the ion in order to represent the screening effect of the ambient plasma.[4,9-19]

The average-atom approach—in addition to the TF calculations that we will discuss below—has been explored more thoroughly. The screened hydrogenic ionization model[20] describes shell populations through a distribution function of occupation numbers which is determined self-consistently. The density-functional theory,[21] in which the free energy of the system is written as a functional of the ion and electron densities and then formal equations are obtained for them variationally, has been adapted to hydrogenic plasmas by Dharmawardana[22] and Perrot.[23] Following the pioneering work of Stewart and Pyatt,[24] and later works by Weisheit and Rozsnyai[25] and Rozsnyai,[26] Skupsky[27] used the screened potential given by the nonlinear Debye-Hückel theory to provide the shifted energy levels of hydrogenic ion impurities in a hydrogen plasma through the solution of the Schrödinger equation. Many aspects of the previous theories have been combined in the work of Davis and Blaha[28] and Cauble, Blaha, and Davis[29] to calculate the fundamental properties of a neon plasma, including the degree of ionization. They solved the Schrödinger equation in a TF-like potential and use occupation numbers based on a Fermi distribution to represent inner-shell effects. In a recent work, Rinker[30-31] solved the Schrödinger equation in a combined TF-like and Hartree-Fock potential for the calculation of transport coefficients over the entire periodic table; the degree of ionization was determined by a generalized Ziman formula.

The Thomas-Fermi statistical model[5–8] combines relative simplicity, clarity, and excellent qualitative descriptive capacity, and it has proven to be a powerful method to calculate the average properties of the atomic system, such as the equation of state and the degree of ionization. The method, originally formulated for isolated, neutral atoms,[8] has been extended in a number of ways to describe plasmas[6,7,20,24–26,32–35] and dense plasma in particular.

Kobayashi[5] solved the zero-temperature Thomas-Fermi equation for positive ions still in the framework of the isolated ion model, and calculated the degree of ionization for arbitrary atomic number as a function of the ionic radius. For finite temperature, Feng and coworkers[36,37] compiled a detailed study of the degree of ionization for a high-density pure hydrogen plasma in the confined Thomas-Fermi[6,7] and Debye-Hückel–Thomas-Fermi[32] (DHTF) approximations, as explained below. The results of Feng's work are shown in Fig. 1.

In the so-called confined-atom TF model,[6,7] each "atom"—consisting of the ion and the free electrons—is assumed to be enclosed in a sphere whose radius is the ion sphere radius without any penetration of the neighboring atoms. Also, due to the neutrality of the sphere there is no interaction between neighboring atoms. Within this model there are two ways to determine the degree of ionization. The first calculates the bound-electron number N_b by integrating the electron distribution function over negative-energy states, then the free-electron number z is given by $z=Z-N_b$ with the atomic number Z. Curve *a* in Fig. 1 shows this result. The second method neglects the polarization of free electrons produced by their attraction toward the nucleus, and gives the free-electron number by $z=(4\pi/3)r_0^3 n(r_0)$, where $n(r_0)$ is the electron density at the atomic boundary r_0. The result from this calculation is shown by curve *e* in Fig. 1.

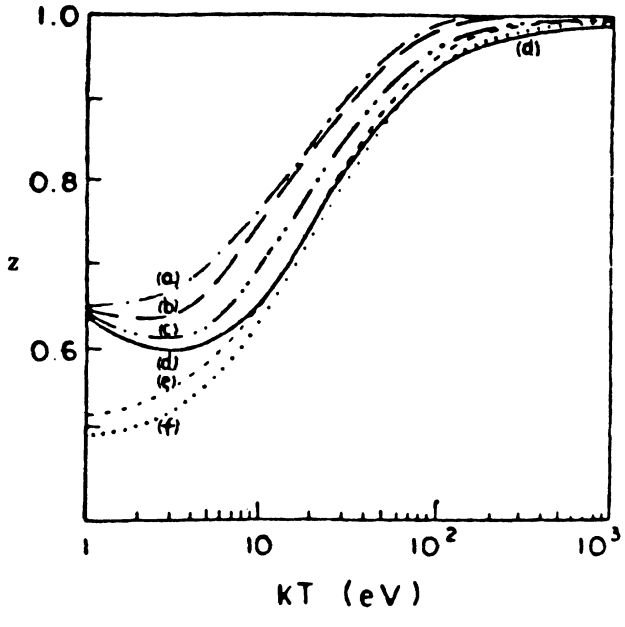

FIG. 1. Average degree of ionization z for a pure hydrogen plasma of ion density $n_i=10^{23}$ cm^{-3} from Feng's paper. (Figure is taken from Ref. 36). Curve (*a*), TF model with integral definition; curve (*b*), DHTF model restricting bound electrons to total energy <-0.1 kT; curve (*c*), DHTF model restricting bound charge to distance less than r_0; curve (*d*), DHTF model with integral definition; curve (*e*), TF model $z=\frac{4}{3}\pi r_0^3 n_e(r_0)$; and curve (*f*), DHTF model, Rozsnyai's approach.

One expects that for a high-density and low-temperature plasma the confined-atom TF model is appropriate. On the other hand, one knows that for a low-density and high-temperature situation the plasma is completely ionized and in such a plasma, if weakly coupled, the Debye-Hückel theory is adequate. In order to describe the intermediate plasma conditions, the DHTF model has been developed to serve as an interpolation between the Debye-Hückel model and TF model. In the DHTF theory, the potential surrounding a test nucleus is generated by both electrons and neighboring ions and the atomic radius is infinite. Here the charge densities are allowed to diffuse into each other's neighborhood and the interaction between neighbors is thus taken into account. Since the DHTF model involves a more complex picture than the TF model, there is a great deal of ambiguity about the definition of the bound electrons. Actually, many different options have been adopted to calculate the ionization. A straightforward way to determine the ionization is to define the bound electrons as the electrons with a negative total energy and calculate the number of bound electrons N_b by integration. Again the number of free electrons z is given by $z=Z-N_b$. Results for this are shown in curve *d* in Fig. 1. An anomalous feature found in this curve that z decreases as temperature increases through low and intermediate temperature for a given density suggests that this definition of bound electrons is improper.

Some attempts have been made to remedy this defect. If the bound electrons are restricted to be inside the ion sphere radius r_0 in addition to having negative energy, the calculation of ionization shows that the above anomalous feature would be diminished, but would still exist (see curve *c* in Fig. 1). In order to reach further improvements, other criteria could be imposed to define the bound electrons differently. For example, a condition that the total energy of bound electrons has to be less than -0.1 kT has been suggested. The result of this calculation is shown by curve *b* in Fig. 1. Here the minimum of z practically disappears. Although a reasonable result has been obtained in this way, the *ad hoc* assumption itself lacks physical justification.

Curve *f* in Fig. 1 is based on a different approach proposed by Rozsnyai and Alder.[33,34] These authors defined a radius of neutrality r' in the DHTF model through

$$4\pi\int_0^{r'} n(r)r^2dr=Z\ ,$$

where $n(r)$ is the electron density in the DHTF model. Then the number of free electrons z is obtained by

$$z=\frac{4\pi}{3}r'^3 n(r')\ .$$

A rather satisfactory result is obtained through this model, but the model itself again seems to lack sufficient physical justification.

None of the above approaches provides a satisfactory extension of the TF theory to plasmas, and even less so to strongly coupled plasmas. The density dependence of the degree of ionization due to the confinement of the atoms by their neighbors is qualitatively well described by the confined-atom TF model, but there is no provision in this approach for screening, either by the free electrons or by the other ions. The DHTF theory describes screening but doesn't account for the confinement effect. In addition, it is well known that for strongly coupled plasmas the screening itself is quite different from the simple DH exponential. Finally, the ambiguities related to the definition of the bound electrons have already been noted.

The purpose of the present paper is to present a more consistent and more satisfactory approach to the application of the TF method to dense plasmas. The objectives of the model,[38] briefly, are (i) to provide a better definition of the bound electrons, (ii) to properly describe the strong correlation effects between ions and between ions and electrons, (iii) to pave the way to the consistent combination of plasma kinetic theory with the TF theory. The main features of our model are as follows.

(1) The bound electrons and free electrons are considered separately. Two different types of distribution functions are used to describe the source densities of the bound and free electrons in the Poisson equation.

(2) A physically reasonable definition of the bound electrons, which differs from any earlier definition, is introduced.

(3) The system is also described as a two-component strongly coupled plasma composed of free electrons and TF ions.

(4) The electron and ion source densities in the Poisson equation are described, respectively, through the ion-ion and ion-electron correlation functions.

(5) In contrast to the original DHTF model,[32] where each ion carries a full nuclear charge Ze, we attribute a more realistic charge to the ion, requiring that this charge be in agreement with the resulting average degree of ionization. Thus the degree of ionization has to be determined self-consistently through iteration.

(6) The average degree of ionization is finally determined from the thermodynamic equilibrium condition, i.e., the minimization of the total free energy of the combined free-electron and ion system.

In this paper a new scheme of the TF equations for strongly coupled plasmas is introduced and some somewhat preliminary calculations of the degree of ionization for a hydrogen plasma based on the model are presented. The calculations involving plasmas with $Z>1$ and more sophisticated calculations where the ion-ion and ion-electron correlations are treated by the hypernetted-chain (HNC) integral equation[39–42] are planned for forthcoming publications.

The remaining part of this paper is arranged as follows. Section II introduces the scheme and the basic equations. Section III deals with the detailed procedure of the numerical calculation and presents the results of the degree of ionization for a hydrogen plasma resulting from a "first-order" model. Section IV develops the model in the second approximation. Again the numerical procedure and the results are presented. In Sec. V, we summarize our work, discuss the features of our results, as well as give a brief description of the future work. Some tedious derivations of important results are relegated to the Appendixes.

II. BASIC EQUATIONS

We write the basic Thomas-Fermi equation as

$$\nabla^2 V_1(r)=4\pi e n_0[V(r)] , \tag{1}$$

$$\nabla^2 V(r)=4\pi e\{n_b[V(r)]+n_f[r,V_1(r)] -zn_i[r,V_1(r)]\} . \tag{2}$$

Here we distinguish between two potentials: $V_1(r)$, created only by the bound-electron density n_b; and $V(r)$, created by all the sources, i.e., in addition to n_b by the free-electron density n_f and by the ion density n_i. The different roles the two potentials play are explained below. z is the average number of free electrons per atom to be determined self-consistently.

In contrast to the customary TF models, we confine the ion within a finite radius r_0 such that the bound-electron density vanishes at r_0. Accordingly, the bound-electron density $n_b[V(r)]$ is given by a momentum cutoff integral of the Fermi-Dirac distribution function as

$$n_b[V(r)] =\frac{8\pi}{h^3}\int_0^{p_m}\frac{p^2}{\exp\{[p^2/2m-eV(r)-\alpha]/kT\}+1}dp , \tag{3}$$

where the cutoff momentum p_m is

$$p_m=\{2me[V(r)-V(r_0)]\}^{1/2} . \tag{4}$$

This definition ensures that the bound-electron density vanishes at the ion boundary and that the maximum energy of the bound electrons is the same everywhere within the ion.

The number density of free electrons $n_f[r,V_1(r)]$ and the number density of neighboring ions $n_i[r,V_1(r)]$ are determined through

$$n_f[r,V_1(r)]=\bar{n}_f[1+g_{e\text{-}i}(r,V_1(r))] , \tag{5}$$

and

$$n_i[r,V_1(r)]=\bar{n}_i[1+g_{i\text{-}i}(r,V_1(r))] . \tag{6}$$

Here $\bar{n}_f$ and $\bar{n}_i$ are the average densities of the free electrons and ions, respectively. Electrical neutrality at infinity requires $\bar{n}_f=z\bar{n}_i$. $g_{e\text{-}i}$ and $g_{i\text{-}i}$ are the pair correlation functions for an electron-ion pair and an ion-ion pair, respectively.

The correlation functions $g_{e\text{-}i}$ and $g_{i\text{-}i}$ are to be determined self-consistently in conjunction with the interaction potential $V_1(r)$. Here we emphasize that in order to avoid double counting of the correlation effect, $g_{e\text{-}i}$ and $g_{i\text{-}i}$ are to be treated as functionals of $V_1(r)$ rather than $V(r)$; the latter plays the role of internal potential for bound electrons only. Ultimately, the calculation of $g_{e\text{-}i}$ and $g_{i\text{-}i}$ has to be done through the equilibrium theory of strongly coupled plasmas. The Singwi-Tosi-Land-Sjolander (STLS) mean-field theory[43–45] is commended by its simplicity, but it is now firmly established that the HNC (Refs. 39–41) and the modified HNC (MHNC) (Refs. 46–48) integral equations can provide a reliable description of strongly coupled plasmas. Thus, even though the HNC is not introduced in this paper, it is the combination of the present method with the HNC that is expected to lead to an accurate formulation of the problem.

III. FIRST APPROXIMATION

In order to explore the implications of the new formulation of the TF theory, we may adopt, in a first approximation, $g_{e\text{-}i}(r)=g_{i\text{-}i}(r)=0$; then Eqs. (5) and (6) give

$$n_f=\bar{n}_f, \quad n_i=\bar{n}_i ,$$

and the electrical neutrality condition becomes $n_f=zn_i$. This means that the free electrons and neighboring ions are both assumed to be uniformly distributed and provide an electrically neutral background only.

The primary purpose of adopting this simplified description is to examine our model with the emphasis on such features as the separation of the bound and free electrons, the innovative definition of the bound electrons, and the minimization process of the free energy.

The potential $V(r)$ surrounding the test nucleus in this approximation is given by

$$\nabla^2 V(r)=4\pi e n_b[V(r)] =4\pi e\frac{8\pi}{h^3}\int_0^{p_m}\frac{p^2}{\exp\{[p^2/2m-eV(r)-\alpha]/kT\}+1}dp , \tag{7}$$

with the boundary conditions

$$V(r_0)=\frac{ze}{r_0}, \quad V'(r_0)=-\frac{ze}{r_0^2}, \quad V(r)=\frac{Ze}{r}, \quad \text{when } r\to 0 , \tag{8}$$

where α is a parameter to be determined (not identical to the chemical potential) and Z is the atomic number. Note that a direct result of Eqs. (7) and (8) is that the bound-electron number within r_0, defined by the integral

$$N_b=4\pi\int_0^{r_0} r^2 n_b(r)dr ,$$

equals $Z-z$ from the Gaussian theorem.

For the purpose of numerical calculation, it is convenient to introduce

$$\Psi(x)=\frac{[\alpha+eV(r)]r}{kTr_0}, \text{ with } x=\frac{r}{r_0} . \tag{9}$$

In terms of the new notations, Eq. (7) is reduced to

$$\Psi''(x)=axJ_{1/2}\left[\frac{\Psi(x)}{x},\Psi(1)\right] , \tag{10}$$

where

$$J_n(x,x_0)=\int_0^{x-x_0} dy\frac{y^n}{\exp(y-x)+1} , \tag{11}$$

and

$$a=\frac{(4\pi e)^2(2m)^{3/2}(kT)^{1/2}r_0^2}{h^3} , \tag{12}$$

and the boundary conditions become

$$\Psi(1)=\frac{\alpha+ze^2/r_0}{kT}, \quad \Psi'(1)=\frac{\alpha}{kT}, \quad \Psi(0)=\frac{Ze^2}{kTr_0} . \tag{13}$$

It is evident that after prescribing the quantities kT, r_0, α, and z, the differential equation (10) and the boundary conditions at $x=1$ in Eq. (13) are all specified. Then, an inward integration of Eq. (10) from $x=1$ to $x=0$ is feasible. The solution at $x=0$, i.e., $\Psi(0)$ will provide the value of Z.

The following physical considerations serve as conditions for the determination of these parameters. First, the physical system of interest in this paper is a pure hydrogen plasma. Thus the input parameters kT, r_0, α, and z must be chosen in such a way that one obtains $Z=1$. Consequently, out of the three adjustable parameters r_0, α, and z due to the condition of $Z=1$, only two are independent. Second, a physically reasonable and consistent model requires that the independent adjustable parameters be determined by the conditions of thermodynamic equilibrium. The equilibrium of the combined bound-electron and free-electron system is characterized by the fact that the total free energy F (consisting of the free energy F_1 of bound electrons and the free energy F_2 of free electrons) exhibits a minimum against the variation of the independent parameters. In other words, these parameters are to be determined by a minimization process of the total free energy.

In terms of the new notations, the free energy of bound electrons is given by

$$F_1=(Z-z)\alpha-\frac{2}{3}\frac{aZkT}{\Psi(0)}\ln\{1+\exp[\Psi(1)]\} \times\int_0^1 dx\,x^2\left[\frac{\Psi(x)}{x}-\Psi(x)\right]^{3/2} +\frac{1}{3}\frac{aZkT}{\Psi(0)}\int_0^1 dx\,xJ_{1/2}\left[\frac{\Psi(x)}{x},\Psi(1)\right] \times[\Psi(x)-\Psi'(1)x-2\Psi(0)] . \tag{14}$$

The derivation of the expression (14) is given in Appendix B.

The free energy of free electrons is obtained from the ideal gas formulas. When $(2\pi mkT)^{3/2}/(h^3 n_f) \gg 1$, the Maxwell-Boltzmann statistics applies, which gives

$$F_2 = -zkT \ln \left[\frac{(2\pi mkT)^{3/2}}{h^3 n_f} \right] - zkT; \tag{15}$$

otherwise, the results from Fermi-Dirac statistics have to be used, which gives

$$F_2 = zkT \left[\frac{\mu}{kT} - \frac{2}{3} \frac{I_{3/2}(\mu/kT)}{I_{1/2}(\mu/kT)} \right], \tag{16}$$

where

$$I_n(x) = \int_0^\infty dy \frac{y^n}{\exp(y-x)+1}, \tag{17}$$

and μ is the chemical potential determined by the normalization condition

$$n_f = \frac{4\pi(2\pi mkT)^{3/2}}{h^3} I_{1/2}\left[\frac{\mu}{kT} \right]. \tag{18}$$

Finally, the total free energy per atom is given by

$$F = F_1 + F_2 + F_0, \tag{19}$$

where F_0 is the free energy contributed from the translational motion of the ion, which is independent of the parameters z, r_0 or α, and therefore irrelevant to the minimization process.

The physical implication of the minimization of the total free energy becomes manifest if we choose z and r_0 as the two independent parameters. In this case, the necessary conditions of minimizing the total free energy can be written as

$$\left.\frac{\partial F}{\partial z}\right|_{r_0} = \left.\frac{\partial F_1}{\partial z}\right|_{r_0} + \left.\frac{\partial F_2}{\partial z}\right|_{r_0} = 0 \tag{20}$$

and

$$\left.\frac{\partial F}{\partial r_0}\right|_z = \left.\frac{\partial F_1}{\partial r_0}\right|_z + \left.\frac{\partial F_1}{\partial r_0}\right|_z = 0. \tag{21}$$

Note that Eq. (20) actually gives the condition of equal chemical potentials for the bound electrons and free electrons. As to Eq. (21), in principle it gives the equality of pressures. However, the first term $\partial F_1/\partial r_0|_z$ is proportional to the pressure of bound electrons, which is zero according to the argument at the end of Appendix A; since F_2 is independent of r_0 [Eq. (15) or (16)], the second term $\partial F_2/\partial r_0|_z$ is also zero. Consequently, $\partial F/\partial r_0|_z$ must be zero.

For practical numerical manipulations, the condition of $Z=1$ is satisfied by prescribing kT, r_0, and α, then adjusting z only. For any given set of kT, r_0 and α values, a computer program can be readily designed to find the correct z with the result of $|Z-1| < 10^{-6}$. Then this leaves r_0 and α as the two independent parameters to be determined by the minimization of the total free energy.

The detailed numerical procedure of the calculation is as follows. First, with a fixed r_0, a run for a variety of different α's is generated. With each α, the corresponding z is determined (z being adjusted to give $Z=1$). In each set of α and z values, the free energies F_1, F_2, and F are evaluated. Note that here F_2 is also a function of z. By comparing the F's for different α's, the minimum value of F is selected. Thus the optimum α and the corresponding z are determined.

To illustrate this procedure, Figs. 2–4 show the curves of F_1/kT, F_2/kT, and F/kT versus α/kT for a fixed r_0 as the ion sphere radius in three different cases: (i) ion density $n_i = 10^{23}$ cm^{-3}, kT = 100 eV; (ii) $n_i = 10^{23}$ cm^{-3}, $kT = 10$ eV; and (iii) $n_i = 10^{23}$ cm^{-3}, $kT = 3$ eV. Figures 5–7 show the curves of z that are determined by the condition of $Z=1$ for a given α versus α/kT in the above three cases. Note that these graphs provide us with instructive information. First, in the cases of $kT = 100$ and 10 eV, we observe that F_1 is a monotonic decreasing function of α and F_2 is a monotonic increasing function of α. This accounts for the appearance of a minimum in the graph of F/kT versus α/kT. Furthermore, from Figs. 5–7, it is clear that the corresponding z value is always a monotonic decreasing function of α for a fixed r_0. Therefore in these two cases the chemical potentials of both bound and free electrons are negative. At a certain point where these two chemical potentials are equal, the total free energy shows a minimum. Second, in the case of $kT = 3$ eV, we observe an opposite trend from the previous cases, i.e., F_1 is an increasing function of α and F_2 is a decreasing function of α. This feature also accounts for the appearance of a minimum in the graph of F/kT versus α/kT. The chemical potentials of both bound and free electrons, however, are positive in this case. Again at certain point where they are equal, the free energy shows a minimum.

It is well known that the chemical potential of an ideal gas of free electrons is negative at high temperatures and positive at low or zero temperatures. Now it is shown that the chemical potential of bound electrons has the same temperature dependence, which makes the minimization process possible.

After having found the α value for a given r_0, in the next step, r_0 is varied and the above procedure is repeated to determine the corresponding α and z values for each specific r_0. Then the free energy F is evaluated as a function of r_0 with the condition $\partial F/\partial\alpha|r_0 = 0$ now already being satisfied. Comparing these resulting F's, and selecting again the minimum, in principle, the optimum r_0 can be determined. The total free energy, however, decreases monotonically with the increasing r_0. This can be attributed to the following fact. The free energy of free electrons, not being an explicit function of r_0, is insensitive to the variation of r_0. On the other hand, the free energy of bound electrons monotonically decreases with increasing r_0. Therefore the monotonic behavior of the free energy of bound electrons dominates the trend of the total free energy. Choosing the ion sphere radius as r_0 is appropriate within this framework. The results of the calculated degree of ionization are given in Fig. 8 and

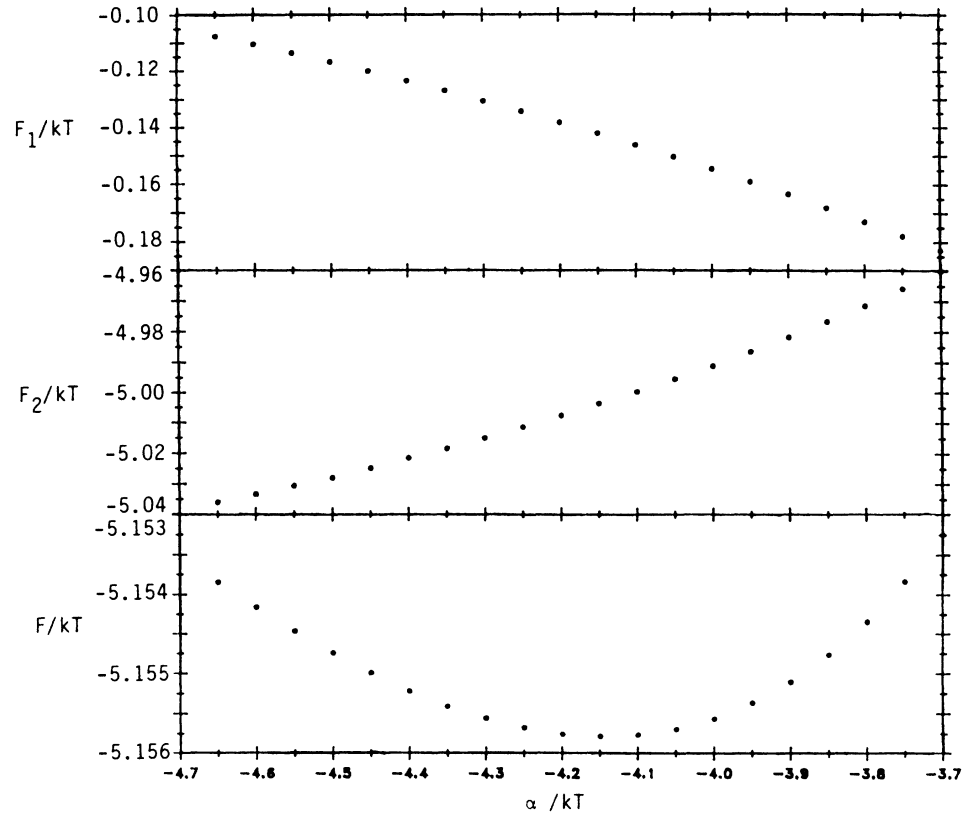

FIG. 2. Free energies F_1/kT, F_2/kT, and F/kT vs α/kT for $n_i = 10^{23}$ cm^{-3} and $kT = 100$ eV in first approximation.

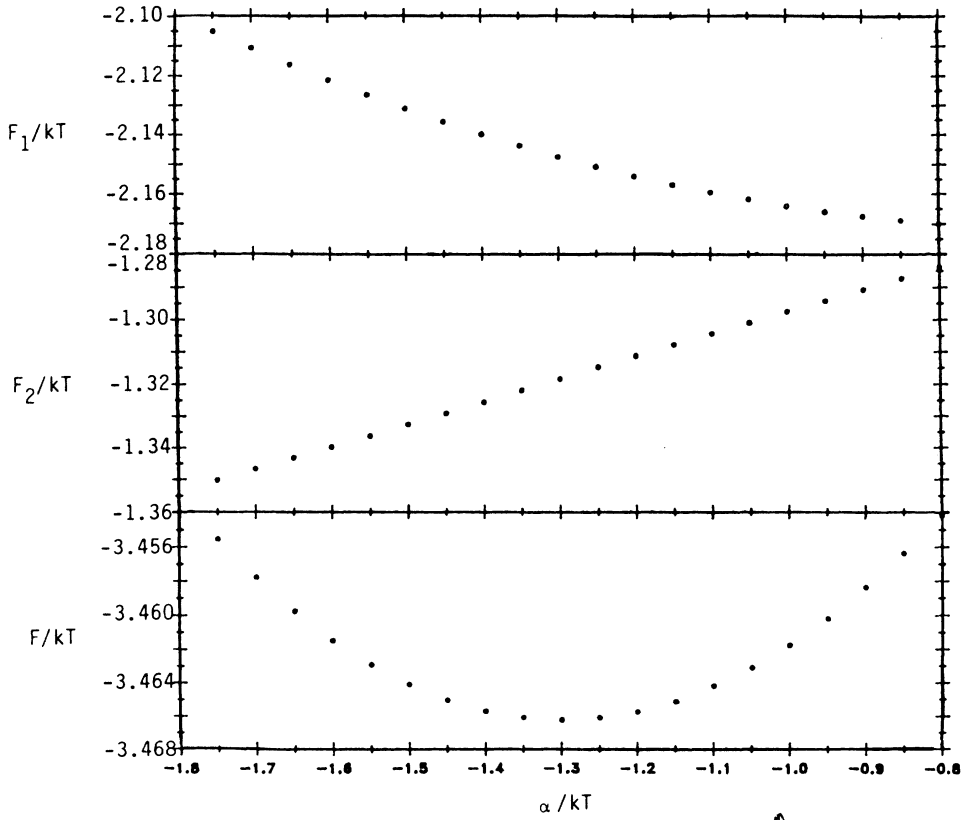

FIG. 3. Free energies F_1/kT, F_2/kT, and F/kT vs α/kT for $n_i = 10^{23}$ and $kT = 10$ eV in first approximation.

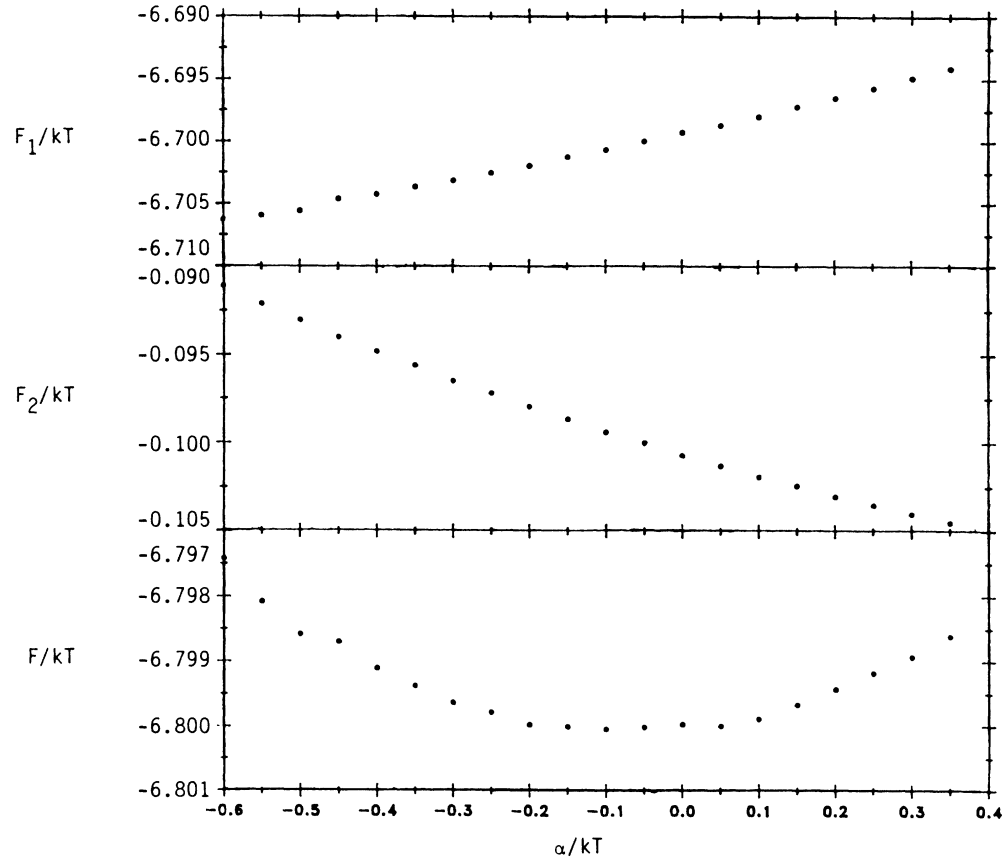

FIG. 4. Free energies F_1/kT, F_2/kT, and F/kT vs α/kT for $n_i=10^{23}$ cm^{-3} and $kT=3$ eV in first approximation.

Table I.

The potential distribution $eV(x)$ inside r_0 in this first approximation in two cases (i) $n_i=10^{23}$ cm^{-3}, $kT=100$ eV and (ii) $n_i=10^{23}$ cm^{-3}, $kT=1$ eV is illustrated in Figs. 9 and 10. For the purpose of further illustration, we also show the radial distribution function $\bar{n}_b(x)$ defined as

$$\bar{n}_b(x)=4\pi r_0^3 n_b(r) \quad \text{with } x=\frac{r}{r_0}\ , \tag{22}$$

where the bound-electron distribution function $n_b(r)$ is given by Eq. (3). $\bar{n}_b(x)$ satisfies a simple normalization relation

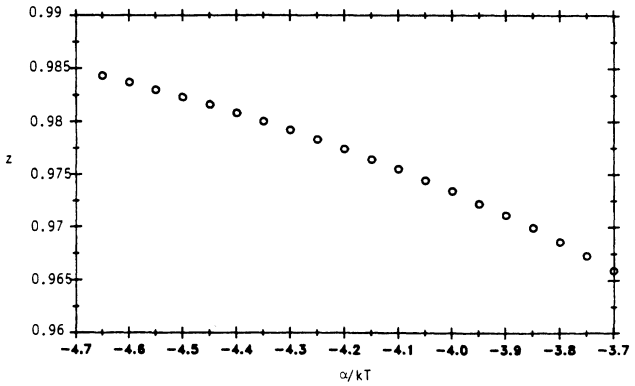

FIG. 5. z vs α/kT for $n_i=10^{23}$ cm^{-3} and $kT=100$ eV in first approximation.

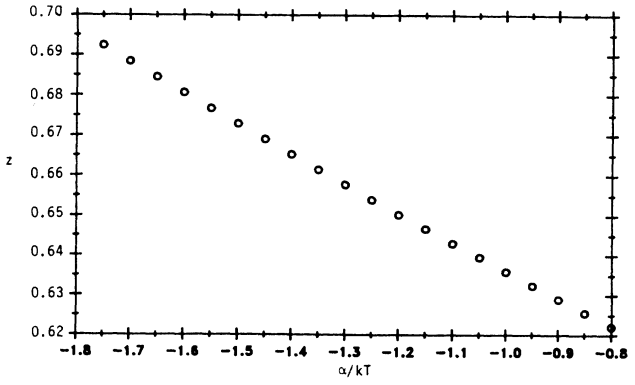

FIG. 6. z vs α/kT for $n_i=10^{23}$ cm^{-3} and $kT=10$ eV in first approximation.

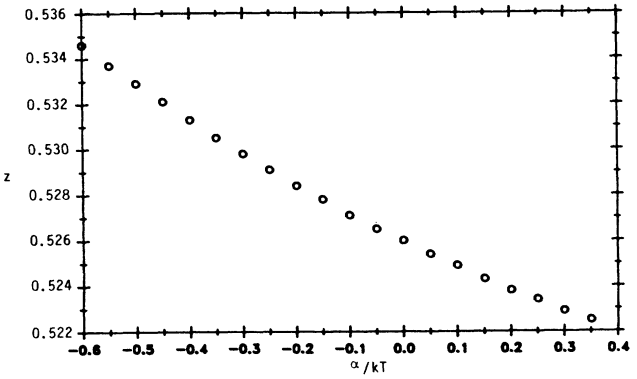

FIG. 7. z vs α/kT for $n_i=10^{23}$ cm^{-3} and $kT=3$ eV in first approximation.

$$\int_0^1 \bar{n}_b(x)x^2dx = N_b = Z - z, \quad \text{with } x = \frac{r}{r_0} . \tag{23}$$

The function $\bar{n}_b(x)$ for the above two cases is plotted in Figs. 11 and 12. In all these graphs we also indicate for comparison the behavior of the confined TF atom, with z being defined as the number of electrons in the positive-energy states.

To complete the presentation of the simplified scheme, we give a brief discussion concerning the zero-temperature limit of this model. At zero temperature, the bound-electron distribution function $n_b(r)$ in Eq. (3) reduces to

$$n_b(r) = \frac{8\pi}{3h^3}\{2me[V(r)-V(r_0)]\}^{3/2} ,$$

$$\text{for } \alpha \geq -V(r_0) = -\frac{ze^2}{r_0} , \tag{24}$$

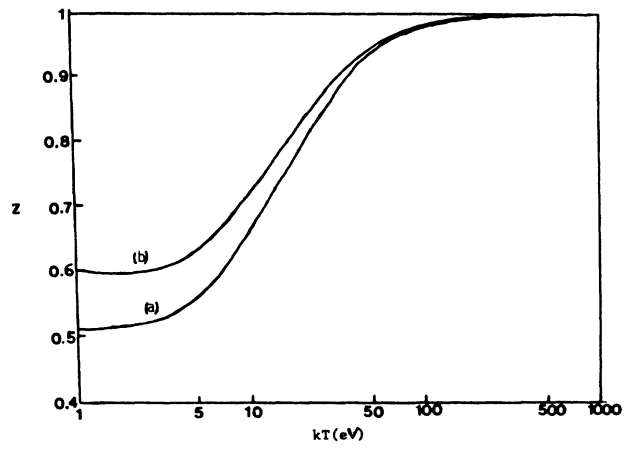

FIG. 8. Average degree of ionization z, for a pure hydrogen plasma of ion density $n_i=10^{23}$ cm^{-3} from the first approximation [curve (*a*)], and second approximation [curve (*b*)].

or

$$n_b(r) = \frac{8\pi}{3h^3}\{2m[eV(r)+\alpha]\}^{3/2} ,$$

$$\text{for } \alpha \leq -V(r_0) = -\frac{ze^2}{r_0} . \tag{25}$$

Therefore, as long as the condition $\alpha \geq -ze^2/r_0$ is satisfied, the TF equation (7) becomes

$$\nabla^2 V(r) = 4\pi e\frac{8\pi}{3h^3}\{2me[V(r)-V(r_0)]\}^{3/2} , \tag{26}$$

with the boundary conditions given in Eq. (8). Note that in this case it recovers the TF equation and the boundary conditions given by Kobayashi[5] for isolated ions at zero temperature.

As it is shown here, if r_0 is given, the parameter α can only be greater than or equal to $-ze^2/r_0$. Suppose α is less than $-ze^2/r_0$; then there exists a radius r_0' defined by $\alpha=-ze^2/r_0'$ such that the density of bound electrons vanishes in the area of $r_0'<r<r_0$ and the actual boundary of the ion would be at r_0' instead of r_0. This outcome is contradictory to the assumption that the ion radius is given by r_0. Therefore we conclude that in the zero-temperature limit our finite-temperature model reproduces the Kobayashi model, as physically expected.

As shown in Kobayashi's paper, the TF equation for isolated ions at zero temperature allows only a one-parameter set of states; that is, when r_0 is specified, the solution for z is uniquely determined. In fact, at certain low temperatures (e.g., at 1 eV with $n_i=10^{23}$ cm^{-3} or at 0.01 eV with $n_i=10^{21}$ cm^{-3}), our finite-temperature model already starts to show the zero-temperature behavior, where when r_0 is fixed, the results of z and all the free energies remain constant, unaffected by the variation of α, provided $\alpha > -ze^2/r_0$. Consequently, we choose this constant z value as the result of the degree of ionization without actually carrying through a minimization process.

Although our finite-temperature model can provide a unique solution for the degree of ionization at the zero-temperature limit, the principle of the minimization of the total free energy fails at this limit, as shown below. One necessary condition for the minimization of the total free energy is that the chemical potentials of the bound electrons and free electrons be equal. The expression for the chemical potential of the bound electrons is given by Eq. (C9) in Appendix C as

$$\mu_1 = \frac{\partial F_1}{\partial(Z-z)}$$
$$= \alpha - \frac{32\pi^2 kT}{3h^3}\ln\left[1+\exp\left[\frac{\alpha+eV_0}{kT}\right]\right]$$
$$\times(2me)^{3/2}\frac{\partial}{\partial(Z-z)}\int_0^{r_0} dr\, r^2[V(r)-V_0]^{3/2} . \tag{27}$$

At the zero-temperature limit, since $\alpha \geq -ze^2/r_0$, from Eq. (24) the total number of bound electrons is

TABLE I. Average degree of ionization for a hydrogen plasma.

n_i (cm^{-3})	kT (eV)	Second approximation	First approximation	Saha equation
10^{23}	10^3	0.9995	0.9994	0.9989
	10^2	0.978	0.9764	0.9647
	10	0.718	0.6577	0.3874
	7	0.670	0.6016	0.2458
	5	0.633	0.5623	0.1384
	3	0.604	0.5273	0.0422
	2	0.595	0.5167	0.0097
	1	0.600	0.5131	
10^{21}	10^3	0.9995	1.0000	1.0000
	10^2	0.997	0.9969	0.9996
	10	0.876	0.8681	0.9622
	7	0.808	0.7886	0.8991
	5	0.726	0.7003	0.7482
	3	0.589	0.5582	0.3348
	2	0.478	0.4522	0.0929
	1	0.317	0.3071	0.0019
10^{19}	10^3	1.000	1.0000	1.0000
	10^2	0.999	0.9994	1.0000
	10	0.962	0.9613	0.9996
	7	0.934	0.9323	0.9987
	5	0.894	0.8912	0.9955
	3	0.798	0.7948	0.9468
	2	0.698	0.6931	0.6094
	1	0.507	0.4994	0.0192

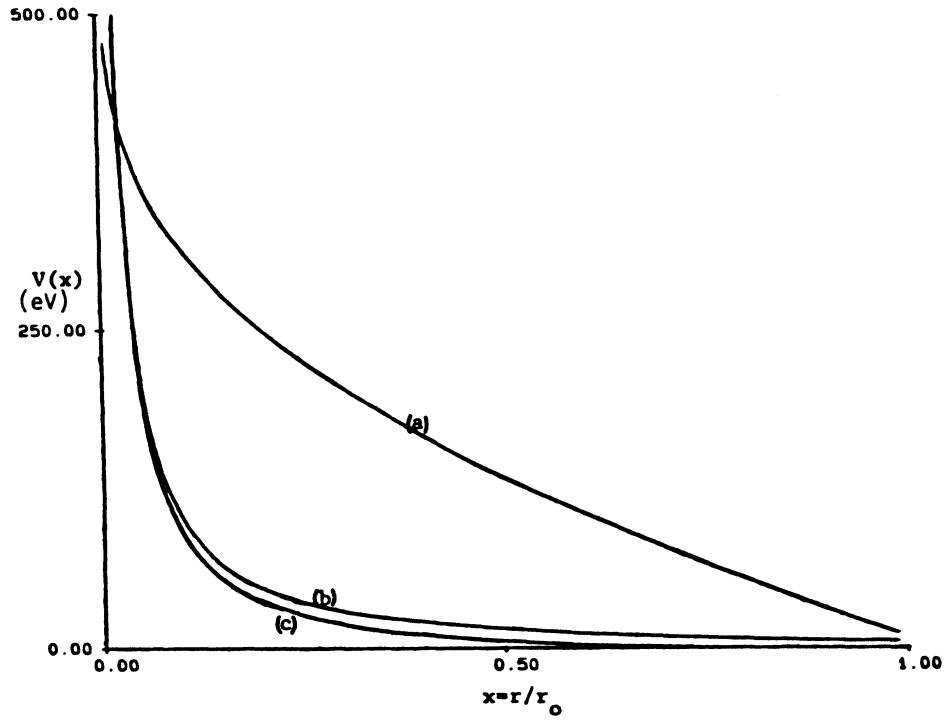

FIG. 9. Potential distribution $V(x)$ inside r_0 for $n_i = 10^{23}$ cm^{-3} and $kT = 100$ eV. Curve (*a*), from first approximation ($\alpha/kT = -4.15$, $z = 0.976$); curve (*b*), from second approximation ($\alpha/kT = -4.15$, $z = 0.978$); and curve (*c*), from TF model for atoms ($\alpha/kT = -4.135$, $z = 0.984$).

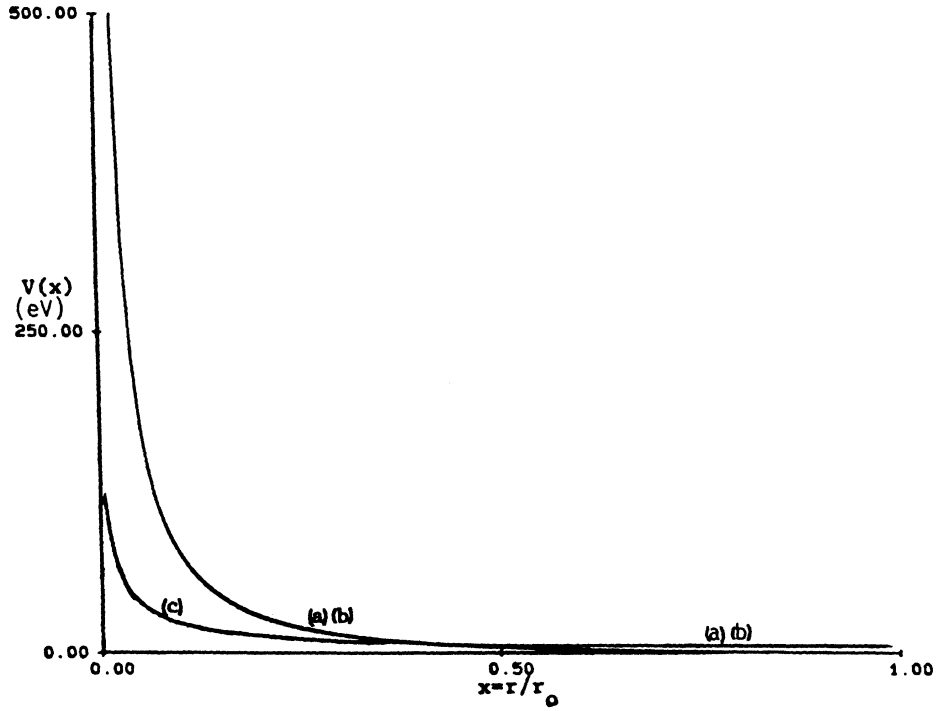

FIG. 10. Potential distribution $V(x)$ inside r_0 for $n_i = 10^{23}$ cm^{-3} and $kT = 1$ eV. Curve (*a*), from first approximation ($\alpha/kT = 5.0$, $z = 0.60$); curve (*b*), from second approximation ($\alpha/kT = 4.853$, $z = 0.657$); and curve (*c*), from TF model for atoms ($\alpha/kT = 4.8$, $z = 0.513$).

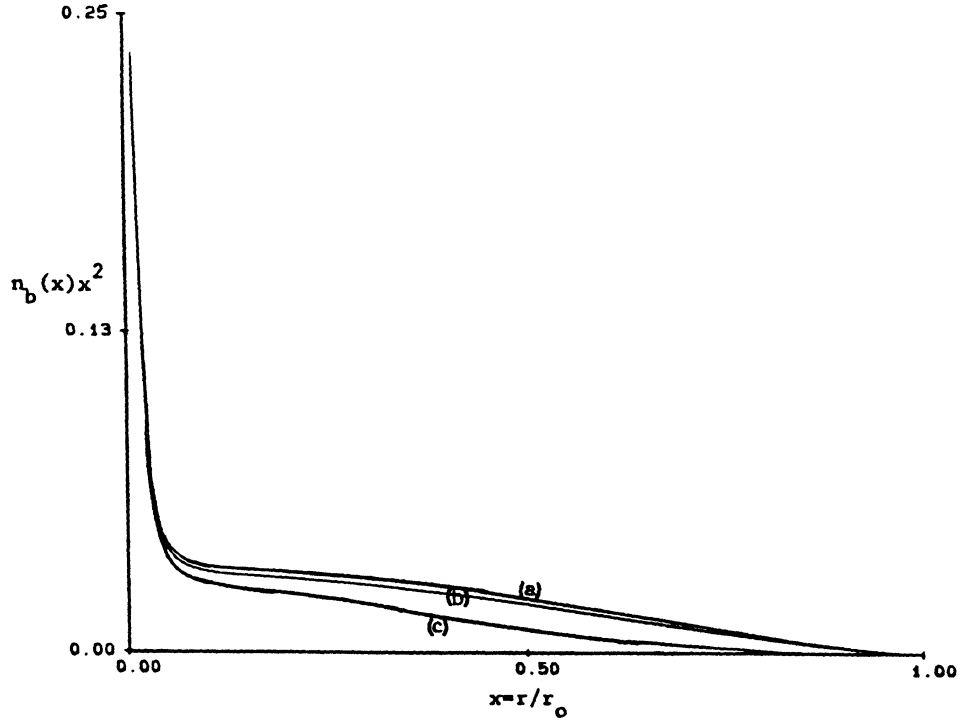

FIG. 11. Distribution function of bound electrons $\bar{n}_b(x)$ inside r_0 for $n_i = 10^{23}$ cm^{-3} and $kT = 100$ eV. Curve (*a*), from first approximation ($\alpha/kT = -4.15$, $z = 0.976$); curve (*b*), from second approximation ($\alpha/kT = -4.15$, $z = 0.978$); and curve (*c*), from TF model for atoms ($\alpha/kT = -4.135$, $z = 0.984$).

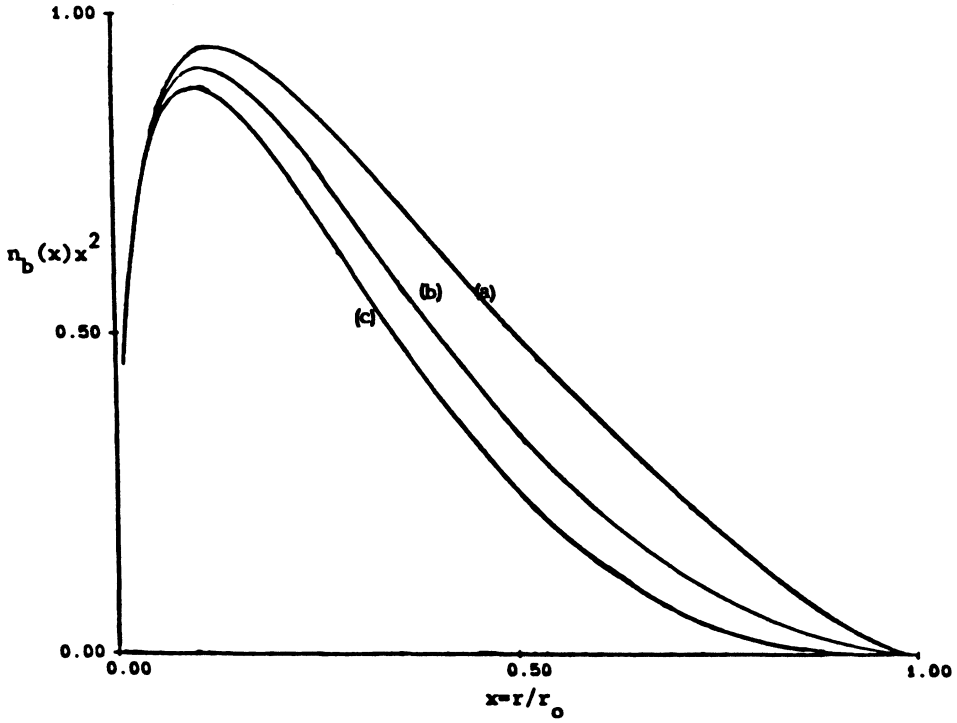

FIG. 12. Distribution function of bound electrons $\bar{n}_b(x)$ inside r_0 for $n_i=10^{23}$ cm^{-3} and $kT=1$ eV. Curve (*a*), from first approximation ($\alpha/kT=5.0$, $z=0.60$); curve (*b*), from second approximation ($\alpha/kT=4.853$, $z=0.657$); and curve (*c*), from TF model for atoms ($\alpha/kT=4.8$, $z=0.513$).

$$Z-z=\frac{32\pi^2}{3h^3}\int_0^{r_0} dr\, r^2\{2me[V(r)-V_0]\}^{3/2}\ . \quad (28)$$

After substituting Eq. (28) for the integral part in Eq. (27), Eq. (27) is reduced to

$$\mu_1=\alpha-kT\ln\left[1+\exp\left[\frac{\alpha+eV_0}{kT}\right]\right]\frac{\partial(Z-z)}{\partial(Z-z)}=-\frac{ze^2}{r_0}\ , \quad (29)$$

which gives a negative value for the chemical potential of bound electrons at zero temperature. Note that at zero temperature $-ze^2/r_0$ is actually the level of the Fermi energy for bound electrons; this result is in agreement with the well-known fact that for a Fermi gas at zero temperature, its chemical potential is equal to its Fermi energy. The chemical potential of free electrons μ_2, on the other hand, is positive at zero temperature; therefore it cannot be the same as the chemical potential of the bound electrons.

It may seem strange that as temperature is lowered from high temperature, the chemical potential of bound electrons μ_1 first changes from negative to positive, then at zero-temperature it becomes negative again. Note that actually at finite temperature the chemical potential of bound electrons μ_1 can be either positive or negative, depending on the value of α. Figures 13–17 show the dependence of μ_1/kT on α/kT in five different cases: (i) $n_i=10^{23}$ cm^{-3}, $kT=7$ eV; (ii) $n_i=10^{23}$ cm^{-3}, $kT=3$ eV; (iii) $n_i=10^{23}$ cm^{-3}, $kT=2$ eV; (iv) $n_i=10^{23}$ cm^{-3}, $kT=1.2$ eV; and (v) $n_i=10^{21}$ cm^{-3}, $kT=1$ eV, where μ_1 is obtained roughly by a difference of the free energy of the bound electrons at different z values. The minimization of the total free energy is accomplished by adjusting the parameter α whenever possible. Apparently, there is a critical temperature $T_{\rm crit}$ near $T=0$ below which μ_1 becomes negative and independent of α, where the minimi-

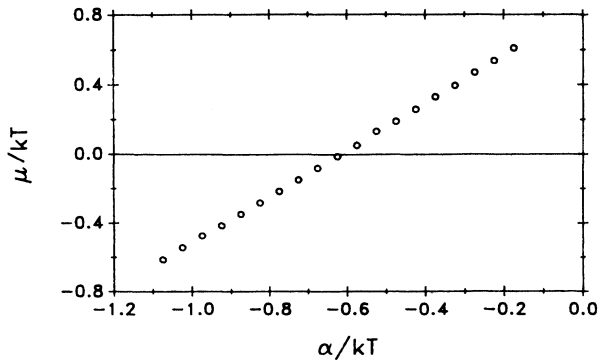

FIG. 13. Chemical potential of the bound electrons μ_1/kT vs α/kT for $n_i=10^{23}$ cm^{-3} and $kT=7$ eV in first approximation.

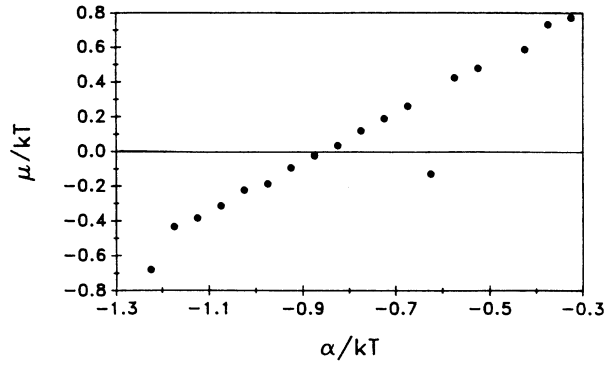

FIG. 14. Chemical potential of the bound electrons μ_1/kT vs α/kT for $n_i=10^{23}$ cm^{-3} and $kT=3$ eV in first approximation.

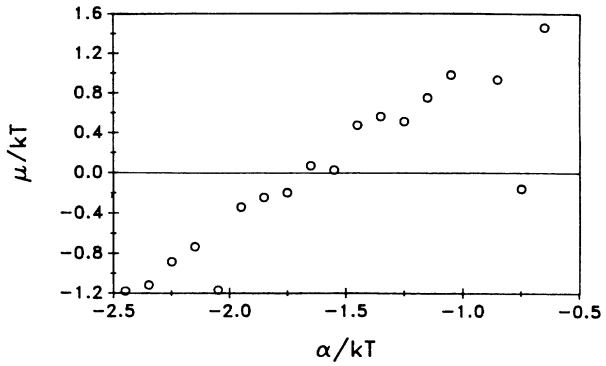

FIG. 16. Chemical potential of the bound electrons μ_1/kT vs α/kT for $n_i=10^{23}$ cm^{-3} and $kT=1.2$ eV in first approximation.

zation fails. The estimated values of the critical temperature is 1 eV for $n_i=10^{23}$ cm^{-3} and 0.1 eV for $n_i=10^{21}$ cm^{-3}. We have not been able to determine the exact values of $T_{\rm crit}$ due to the limitation of the numerical accuracy. Thus, while for $T>T_{\rm crit}$, there is a shared $\mu_1=\mu_2$ chemical potential for the equilibrium system, which changes from negative to positive when temperature is lowered, for $T<T_{\rm crit}$, μ_1 represents the chemical potential of the isolated ion, which is negative.

Some further comments on the relationship between the parameter α and the chemical potential μ_1 are in order. Figures 13–17 show that $\mu_1>\alpha$ holds. The origin of the difference between μ_1 and α can been seen by analyzing the fictitious bound-electron number

$$\tilde{N}_b=\frac{32\pi^2}{3h^3}2me^{3/2}\int_0^{r_0}dr\,r^2[V(r)-V(r_0)]^{3/2}\ ,$$

figuring in Eq. (C8), which is formally identical to the expression for the bound-electron number at zero temperature. While evidently for the actual bound-electron number $N_b=Z-z$, $\partial N_b/\partial z<0$, one can show that $\partial\tilde{N}_b/\partial z>0$. As z increases and N_b decreases, the potential distribution inside the ion opens up (cf. Figs. 9 and 10), deviating from the highly screened atomic potential and approaching the pure Coulomb Ze/r potential. This effect is more important than the concomitant increase of $V(r_0)$. The result is an increase of $V(r)-V(r_0)$ and $\tilde{N}_b$. The difference between N_b and $\tilde{N}_b$ is due, of course, to the fact that the Fermi distribution at finite temperature is quite different from the zero-temperature step-function distribution.

IV. SECOND APPROXIMATION

In the first approximation, we adopted $g_{e\text{-}i}=g_{i\text{-}i}=0$. While the uniformly distributed free-electron model (i.e., $g_{e\text{-}i}=0$) is a reasonable assumption for a high-density plasma, the ion-ion correlation may be quite strong, requiring a more adequate modeling of $g_{i\text{-}i}$. Therefore in our second approximation, a nonlinear Debye-type exponential expression for the ion-ion correlation function is chosen

$$g_{i\text{-}i}=\exp\left[\frac{-zeV(r)}{kT}\right]-1\ . \tag{30}$$

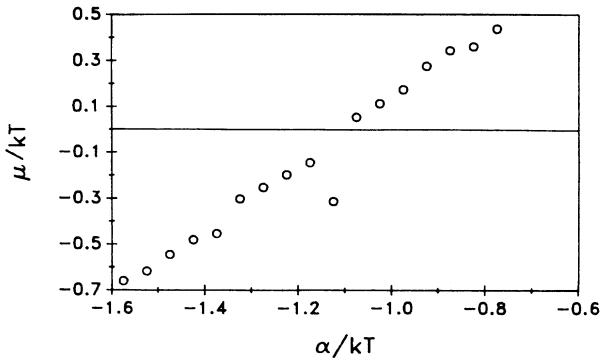

FIG. 15. Chemical potential of the bound electrons μ_1/kT vs α/kT for $n_i=10^{23}$ cm^{-3} and $kT=2$ eV in first approximation.

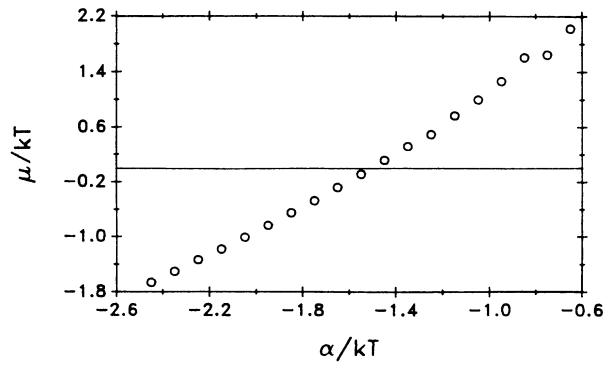

FIG. 17. Chemical potential of the bound electron μ_1/kT vs α/kT for $n_i=10^{21}$ cm^{-3} and $kT=1$ eV in first approximation.

In contrast to Eq. (6), where the ion-ion correlation function $g_{i\text{-}i}$ is a functional of $V_1(r)$, the expression for $g_{i\text{-}i}$ here is a functional of $V(r)$. This is not in contradiction to what has been said there, since using $V(r)$ instead of $V_1(r)$ is precisely the essence of the Debye approximation.

This ion-ion correlation function, though simple, can well describe the main features of correlation. It enables one to examine the ion-ion correlation effect without running into the complexity of the mean-field theory or the HNC integral equation.

Now the Thomas-Fermi equation becomes

$$\nabla^2\nabla(r)=4\pi e\left[\frac{8\pi}{h^3}\int_0^{p_m}\frac{p^2}{\exp\{[p^2/2m-eV(r)-\alpha]/kT\}+1}dp+4\pi ezn_i\right]-4\pi ezn_i\exp\left[-\frac{zeV(r)}{kT}\right], \tag{31}$$

with the boundary conditions

$$V(\infty)=0,\quad V'(\infty)=0,\quad V(r)=\frac{Ze}{r},\quad \text{when } r\to 0\ . \tag{32}$$

The potential and charge distributions around the test nucleus are to be determined by Eq. (31). Note that Eq. (31) is modeled on an extended structure of the central ion, whereas in the same equation the surrounding ions are treated as point charges without inner structure.

The integration of Eq. (31) has to be performed in two different regions: $r_0\le r<\infty$ and $0\le r\le r_0$, separately. In the first region $r_0\le r<\infty$, the bound-electron density vanishes. Using the boundary conditions at infinity, an inward integration from ∞ to r_0 is carried out.

The solution of Eq. (31) at r_0 provides the boundary conditions $V(r_0)$ and $V'(r_0)$ for the integration in the second region $0\le r\le r_0$, as well as the necessary information about $V(r_0)$ in the expression for the bound-electron density. In the first region the differential equation has the form

$$\nabla^2V(r)=4\pi ezn_i-4\pi ezn_i\exp\left[-\frac{zeV(r)}{kT}\right], \tag{33}$$

which is simply the nonlinear Debye equation.

Defining the function

$$\frac{\Psi_1(x)}{x}=\frac{eV(r)}{kT}\ , \tag{34}$$

where

$$x=\frac{r}{r_0}\ , \tag{35}$$

Eq. (33) becomes

$$\Psi_1''=\frac{4\pi ze^2r_0^2n_ix}{kT}\left[1-\exp\left[-\frac{z\Psi_1(x)}{x}\right]\right]. \tag{36}$$

For sufficiently large r, the nonlinear Debye equation (33) reduces to the linear Debye equation

$$\nabla^2V(r)=\frac{4\pi z^2e^2n_i}{kT}V(r)\ , \tag{37}$$

or in terms of the new notations

$$\Psi_1''(x)=\kappa^2\Psi_1(x),\quad \text{where } \kappa^2=\frac{4\pi z^2e^2r_0^2n_i}{kT}\ . \tag{38}$$

Incorporating the boundary conditions

$$\Psi_1(\infty)=0,\quad \Psi_1'(\infty)=0\ , \tag{39}$$

Eq. (36) has the solution

$$\Psi_1(x)=ce^{-\kappa x},\quad \Psi_1'(x)=-c\kappa e^{-\kappa x}=-\kappa\Psi_1(x)\ , \tag{40}$$

where c is a normalization constant.

With prescribed c and z, at some large x, Eq. (40) actually provides the boundary conditions that Eq. (36) should meet. Therefore, with prescribed c and z, Eq. (36) can be integrated from a large x to 1 and its solution $\Psi_1(1)$ and $\Psi_1'(1)$ is used in the following.

In the domain $0\le r\le r_0$, the new notations defined in Eq. (9) are used again and Eq. (31) becomes

$$\Psi''(x)=axJ_{1/2}\left[\frac{\Psi(x)}{x},\Psi(1)\right]+\frac{4\pi ze^2r_0^2n_ix}{kT}\times\left\{1-\exp\left[-z\left[\frac{\Psi_1(x)}{x}-\frac{\alpha}{kT}\right]\right]\right\}, \tag{41}$$

and the boundary conditions at $x=1$ are related to the previously calculated $\Psi_1(1)$ and $\Psi_1'(1)$ by

$$\Psi(1)=\Psi_1(1)+\frac{\alpha}{kT},\quad \Psi'(1)=\Psi_1'(1)+\frac{\alpha}{kT}\ . \tag{42}$$

Another boundary condition $\Psi(x)$ must meet is

$$\Psi(0)=\frac{Ze^2}{r_0kT}\ . \tag{43}$$

Again the α here is a constant to be determined and not identical to the chemical potential.

Evidently, there are three parameters here, c, z, and α, that have to be determined. The conditions for determining them are (i) the solution of Eq. (41) at $x=0$, i.e., $\Psi(0)$ should meet the boundary condition given by Eq. (43), (ii) the prescribed z in the differential equation (31) should be the same as the z obtained from the resulting bound-electron number N_b by the relation $z=Z-N_b$; (iii) the total free energy of the combined bound-electron, free-electron and ion system should exhibit a minimum against the variation of the adjustable parameters.

In order to satisfy these conditions we proceed as follows. First, for any given z and α, parameter c is to be chosen in such a way that the solution of Eq. (41) at $x=0$

gives $Z=1$. A computer program is designed to adjust c and to meet the requirement of $|Z-1|\leq 10^{-5}$ automatically. Next an evaluation of the bound-electron number N_b is carried out. N_b is given by the integral

$$N_b=4\pi\int_0^{r_0} r^2 n_b(r)dr \ . \tag{44}$$

This leads to a new value of z, which, in general, is different from the one prescribed. Therefore an iteration is needed to obtain a self-consistent z. The output z is put back into the differential equation and the entire procedure is repeated. The iteration continues until z converges to within the desired accuracy. (The difference between a pair of successive z values is required to be less than 10^{-5}.) Note that in each step of the iteration, a new c must be selected.

Finally, the parameter α has to be determined through the minimization of the free energy. The total free energies evaluated for different α values are compared and the minima are to be selected. Note that for each α in the sequence, the corresponding c and self-consistent z must be determined by the procedure described above.

The determination of the total free energy of the combined ion and free-electron system in the framework of this second approximation is given in Appendix D.

To illustrate the procedure of the minimization of the total free energy, Figs. 18–20 show the curves of $F_{\rm tot}/kT$ versus α/kT in three different cases: (i) ion density $n_i=10^{23}$ cm^{-3}, $kT=1000$ eV; (ii) $n_i=10^{23}$ cm^{-3}, $kT=100$ eV; and (iii) $n_i=10^{23}$ cm^{-3}, $kT=1$ eV. The minima of the total free energy are marked on the graphs.

The results of the calculated degree of ionization from this model and the first approximation are given in Fig. 8 and Table I. The results from the Saha-equation approach[1] are also given in Table I. Comparison of our results with the results from the Saha equation shows that, for a given density at sufficiently high temperatures (depending on the ion density), the degree of ionization calculated from the Saha equation is higher than ours; whereas, at low temperatures, the one from the Saha equation is lower than ours.

The potential distribution $eV(x)$ inside r_0 from this calculation in two cases (i) $n_i=10^{23}$ cm^{-3}, $kT=100$ eV and (ii) $n_i=10^{23}$ cm^{-3}, $kT=1$ eV is also illustrated in Figs. 9 and 10 (curve *b*) together with the one from the first approximation (curve *a*). For further comparison, the potential distribution $eV(x)$ inside r_0 from the original finite-temperature TF model for neutral atoms[6,7] is illustrated in Figs. 9 and 10 as well (curve *c*).

These three graphs show that the potential has the highest value according to the first approximation and the lowest value according to the original TF model. This feature can be explained by considering the degree of ion penetration, which tends to increase the value of $eV(x)$. In the first approximation, ions are assumed to be uniformly distributed, which represents the highest degree of ion penetration. In the second approximation, the

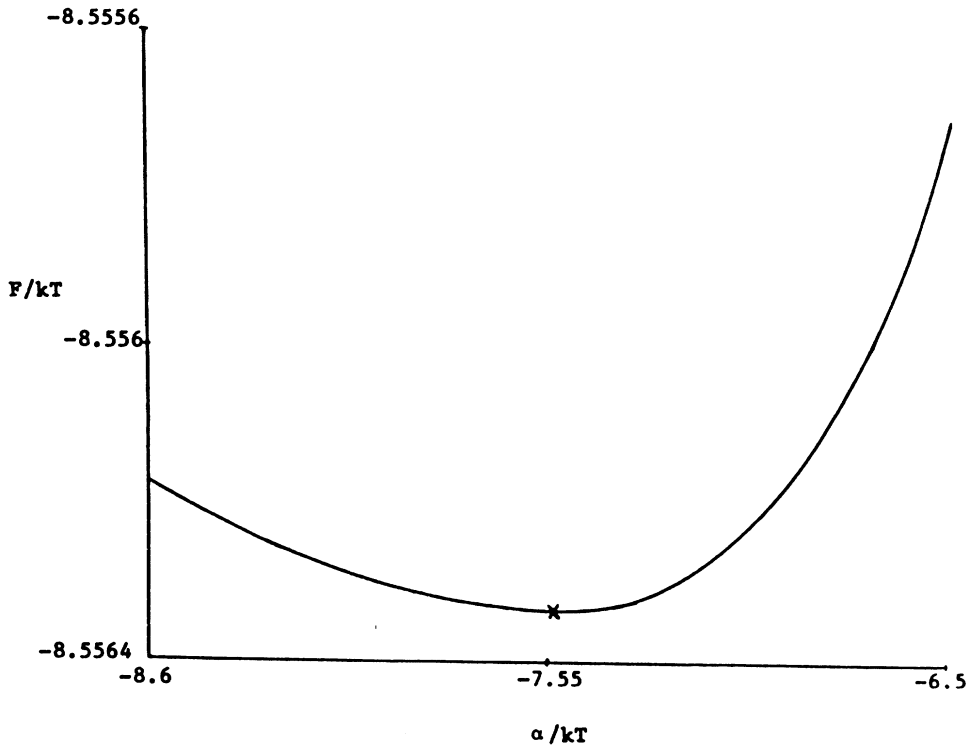

FIG. 18. Free energy F/kT vs α/kT for $n_i=10^{23}$ cm^{-3} and $kT=1000$ eV in second approximation.

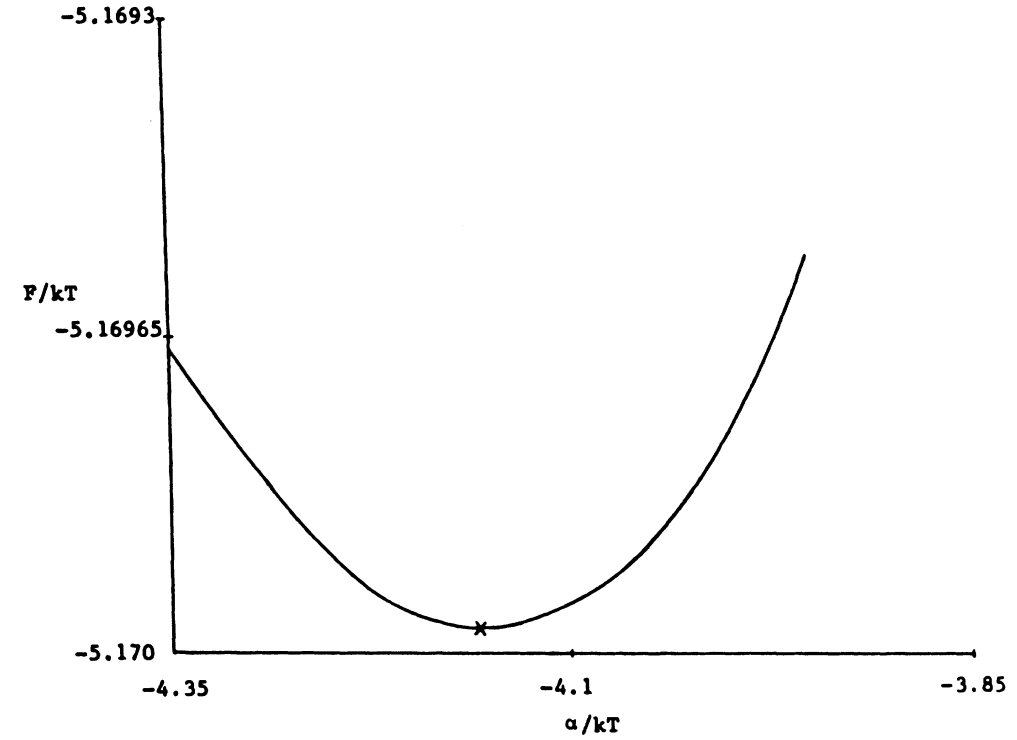

FIG. 19. Free energy F/kT vs α/kT for $n_i = 10^{23}$ cm^{-3} and $kT = 100$ eV in second approximation.

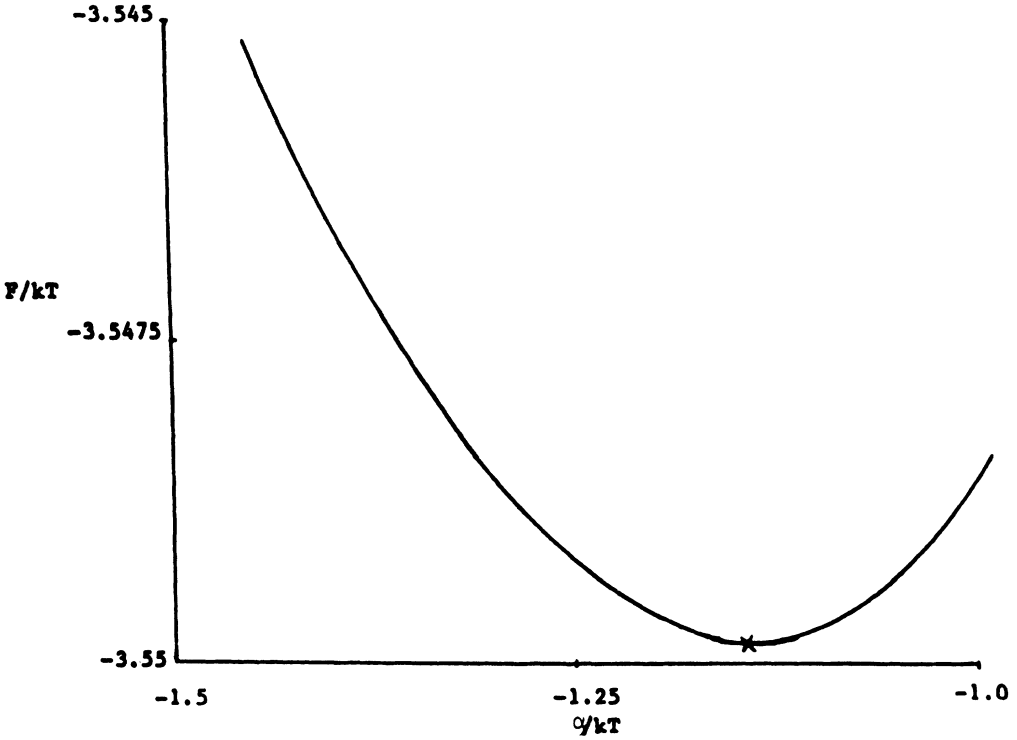

FIG. 20. Free energy F/kT vs α/kT for $n_i = 10^{23}$ cm^{-3} and $kT = 10$ eV in second approximation.

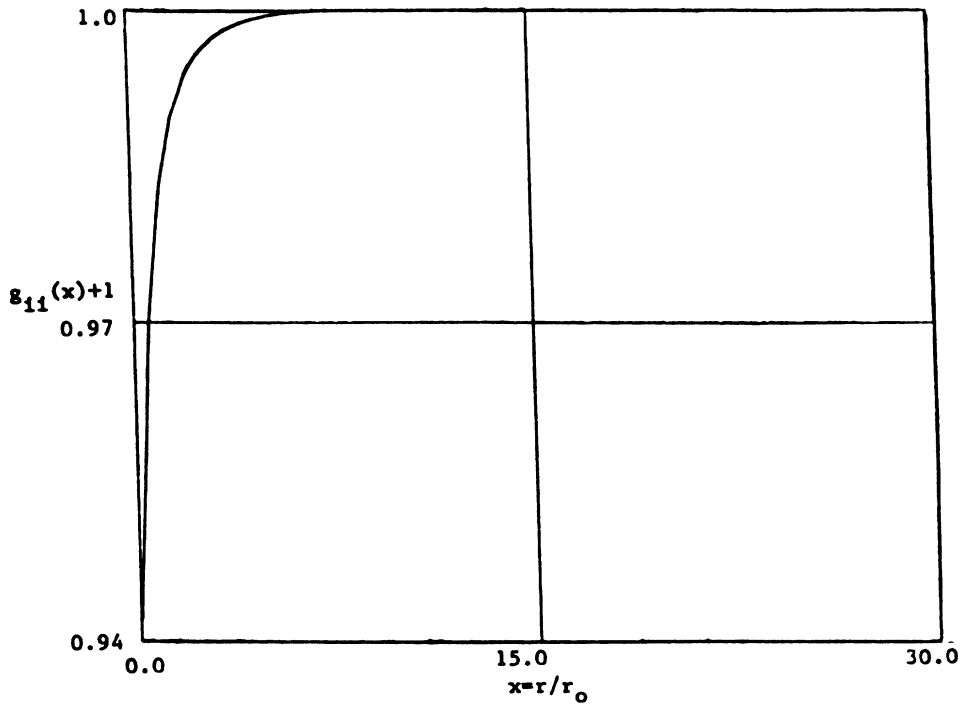

FIG. 21. Ion distribution function $[g_{i\text{-}i}(x)+1]$ in second approximation for $n_i=10^{23}$ cm^{-3} and $kT=100$ eV.

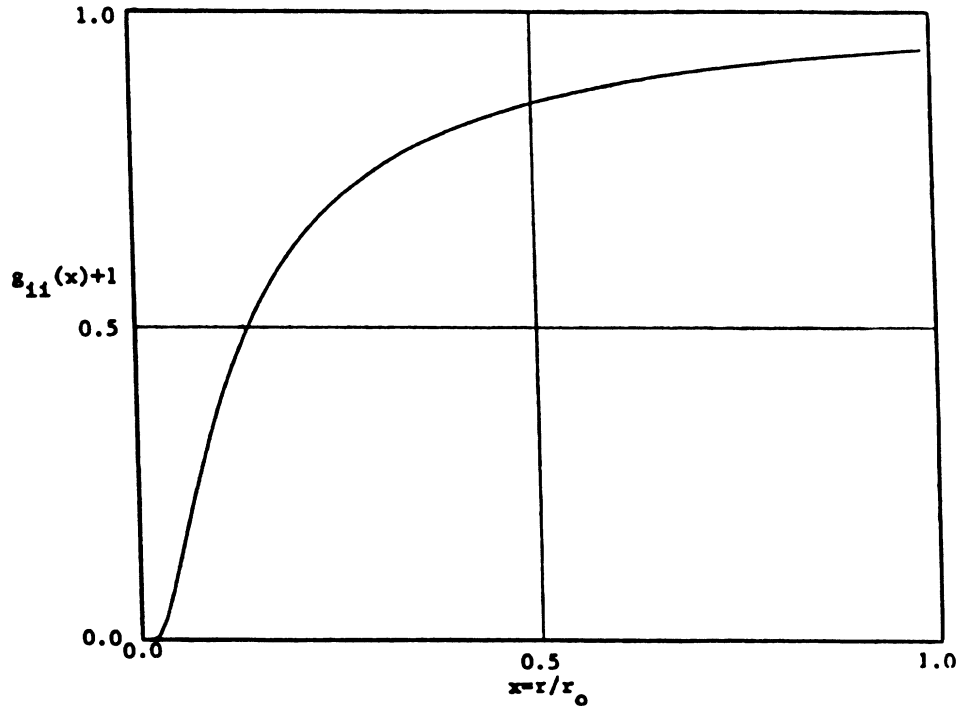

FIG. 22. Ion distribution function $[g_{i\text{-}i}(x)+1]$ inside r_0 in second approximation for $n_i=10^{23}$ cm^{-3} and $kT=100$ eV.

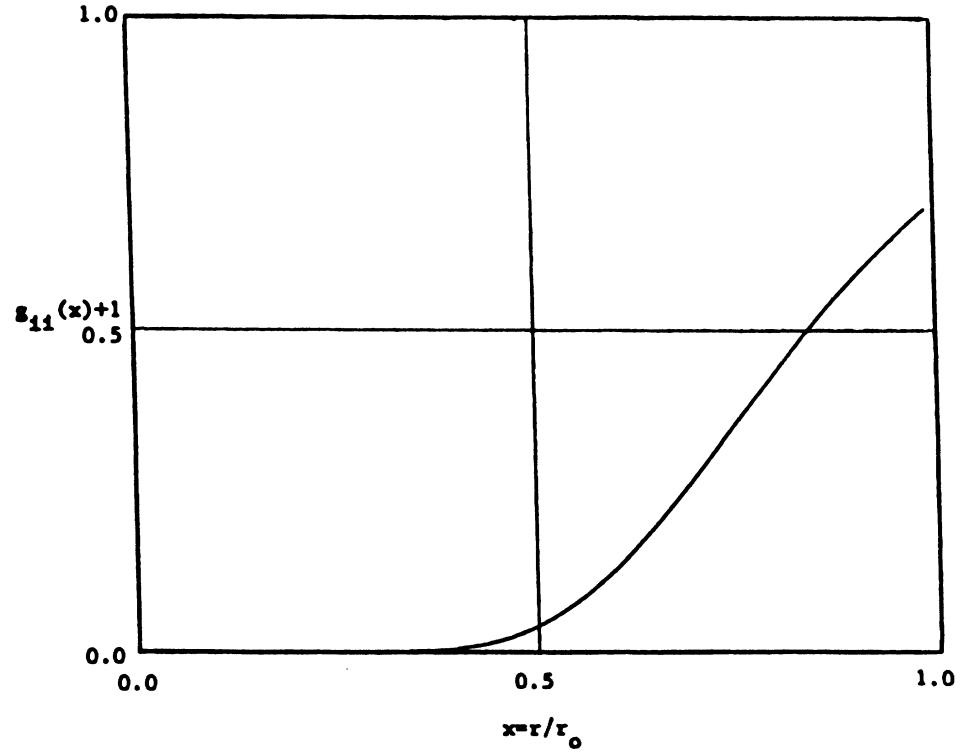

FIG. 23. Ion distribution function $[g_{i\text{-}i}(x)+1]$ inside r_0 in second approximation for $n_i=10^{23}$ cm^{-3} and $kT=1$ eV.

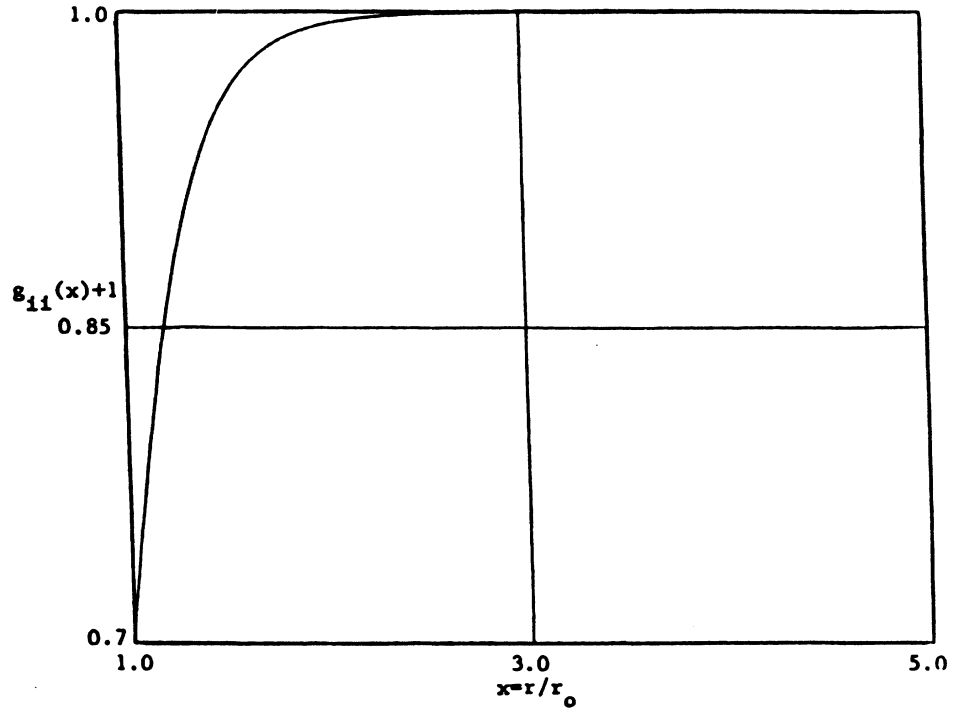

FIG. 24. Ion distribution function $[g_{i\text{-}i}(x)+1]$ outside r_0 in second approximation for $n_i=10^{23}$ cm^{-3} and $kT=1$ eV.

ion-ion correlation function is expressed by a nonlinear Debye distribution function. Here the ion penetration exists, but the correlation effect between ions keeps them apart, i.e., the ion penetration is weaker than in a uniform distribution. In the confined TF model, atoms are enclosed in spheres with radius r_0 without penetrating each other at all.

In Figs. 9 and 10, we may also note the different values of $eV(r)$ at $r=r_0$ $(x=1)$. In the first approximation the value of $eV(r_0)$ is equal to ze^2/r_0. In the confined TF model, the value of $eV(r_0)$ is zero, in agreement with the neutral atom picture of this model. Finally, in the second approximation, due to the reduced ion penetration $eV(r_0)<ze^2/r_0$.

The bound-electron distribution functions $\bar{n}_b(x)$ defined by Eq. (22) as resulting from the present calculation, both in the first and second approximations, and from the original TF model, where bound electrons are defined as having negative total energy, are illustrated in Figs. 11 and 12. The ion distribution functions $[g_{i\text{-}i}(x)-1]$ inside and outside r_0 are illustrated in Figs. 21–24.

V. CONCLUSIONS

In this paper we have presented a different version of the TF theory for ions embedded in a plasma. This model is expected to be a more adequate description of a strongly coupled plasma, consisting of strongly coupled ions and strongly coupled electrons, than earlier attempts, for several reasons.

First, we have provided a unique and unambiguous definition of the bound electrons, which is probably the best description, within the TF model, of the vanishing bound-electron wave function on the boundary of the ion in the exact quantum-mechanical description. In previous works,[36,37] the difficulty and the unphysical results in the calculation of the degree of ionization mainly came from the improper definition of bound electrons. The theory of continuum lowering and pressure ionization suggests that the electrons at the ion boundary should be all considered to be in the continuum. Moreover, the results of the calculated degree of ionization, both in the first and second approximations of the model, have eliminated the unphysical dip that appeared in the degree of ionization versus kT curves in the previous works.[36,37] This favorable feature also indicates that a reasonable definition of bound electrons has been adopted.

Second, we have used a thermodynamically correct, self-consistent minimization procedure to determine the degree of ionization of the plasma, rather than calculating it solely from the properties of the isolated ion. It is, of course, precisely the minimization of the free energy that leads to the conventional Saha-equation approach, but this is the first time that such a scheme ever succeeds in the framework of the TF model. This feature renders the present model a more reliable and thermodynamically consistent approach to the ionization equilibrium problem than those used previously.

Third, we have used the correlation function between the test ion and the surrounding plasma particles to describe their penetration into the test ion; this is certainly more satisfactory than the *ad hoc* linearized Debye or excluded-volume approach. At the same time, we have consistently included the ion-ion correlation in the determination of the free energy of the system, which ensures that the effect of the correlation, including depression of the continuum on the ionization, is automatically accounted for. Again, this is the first time that the effect of correlations both on the bound states and on the thermodynamics of the system is simultaneously taken into account in the framework of the TF approximation. Furthermore, comparing the results from the first and second approximations of the model reveals the effect of the ion-ion correlations. We note that the value of the degree of ionization in the second approximation is greater than in the first approximation. This is because the effect of the ion-ion correlation is to reduce the ion density in the vicinity of the ion of interest, which in turn makes the binding potential weaker for the bound electrons. Therefore, in the second approximation, fewer electrons can be bound, resulting in a higher degree of ionization.

Fourth, inherent in our model is the recognition of the fact that while each ion develops an electrostatic potential on its surface, the average of the rapidly fluctuating potential in the plasma is zero because of the quasineutrality of the system. This is the basic assumption of the conventional plasma kinetic theory and it allows the use of systematic calculation of particle distribution and correlation functions.

The calculated degree of ionization for hydrogen moves away from the simplistic Saha-equation result in a physically reasonable way without the inherently disadvantageous features or arbitrariness of the earlier TF approach. However, both the scarcity of existing experimental data and the fact that hydrogen is not the prime candidate for the application of the TF approximation make it unrealistic to seek quantitative experimental corroboration of our data. In future works the application of the model to the high-Z plasma is planned to be carried out in conjunction with using the far more adequate HNC integral equation to determine the strong ion-ion correlations, and eventually, the electron-ion correlation as well. With the accumulation of experimental data[49] and with the quantitative improvement of the model, a comparison between the theory and observation should become possible. At this point one can decide whether further improvement of the model by inclusion of the more conventional exchange, correlational gradient, etc.,[20] corrections is warranted.

ACKNOWLEDGMENTS

We acknowledge useful discussions with Jack Davis and Guoping Zhou. This work has been partially supported by the National Science Foundation, under Grant Nos. ECS-87-13337 and ECS-83-15655.

APPENDIX A: VERIFICATION OF THE VIRIAL THEOREM

The virial theorem, an important statement on the relationship between the kinetic energy and potential energy of the ion, can be derived in the framework of the scheme presented here.

The kinetic energy of the ion is

$$E_{\rm kin}=\frac{32\pi^2}{h^3}\int_0^{r_0}r^2dr\int_0^{p_m}\frac{p^2(p^2/2m)}{\exp\{[p^2/2m-eV(r)-\alpha]/kT\}+1}dp\ , \tag{A1}$$

or, in terms of the new notations,

$$E_{\rm kin}=\frac{aZkT}{\Psi(0)}\int_0^1 dx\,x^2J_{3/2}\left[\frac{\Psi(x)}{x},\Psi(1)\right], \tag{A2}$$

which can be reduced through integration by parts to

$$E_{\rm kin}=-\frac{aZkT}{3\Psi(0)}\int_0^1 dx\,x^3\frac{d}{dx}J_{3/2}\left[\frac{\Psi(x)}{x},\Psi(1)\right]. \tag{A3}$$

Noting that

$$\frac{d}{dx}J_{3/2}(x,x_0)=\tfrac{3}{2}J_{1/2}(x,x_0)\ , \tag{A4}$$

and substituting Eq. (A4) into Eq. (A3) yield

$$\begin{aligned}E_{\rm kin}&=-\frac{aZkT}{2\Psi(0)}\int_0^1 dx\,x^3\left[\frac{\Psi'(x)}{x}-\frac{\Psi(x)}{x^2}\right]J_{1/2}\left[\frac{\Psi(x)}{x},\Psi(1)\right]\\&=-\frac{aZkT}{2\Psi(0)}\left[\int_0^1 dx\,\Psi(x)\Psi''(x)-\int_0^1 dx\,x\Psi'(x)\Psi''(x)\right]\\&=\frac{ZkT}{2\Psi(0)}\left[\Psi(1)\Psi'(1)-\Psi(0)\Psi'(0)-\tfrac{1}{2}\int_0^1 dx\,[\Psi'(x)]^2-\tfrac{1}{2}[\Psi'(1)]^2\right].\end{aligned} \tag{A5}$$

The potential energy of the ion includes two parts,

$$E_{\rm pot}=E_{e\text{-}e}+E_{e\text{-}n}\ , \tag{A6}$$

where $E_{e\text{-}e}$ is the potential energy resulting from the mutual interaction between the electrons, and $E_{e\text{-}n}$ is the one resulting from the interaction between the electrons and nucleus.

The two terms in Eq. (A6) are given by

$$E_{e\text{-}e}=-\tfrac{1}{2}4\pi e\int_0^{r_0}r^2dr\,n(r)V_e(r) \tag{A7}$$

and

$$E_{e\text{-}n}=-4\pi e\int_0^{r_0}r^2dr\,n(r)V_n(r)\ , \tag{A8}$$

where

$$V_e(r)=-4\pi e\int_0^{r_0}r'^2dr'\frac{n(r')}{|\mathbf{r}-\mathbf{r}'|}\ , \tag{A9}$$

$$V_n(r)=\frac{Ze}{r}\ , \tag{A10}$$

and

$$n(r)=\frac{8\pi}{h^3}\int_0^{p_m}\frac{p^2}{\exp\{[p^2/2m-eV(r)-\alpha]/kT\}+1}dp\ . \tag{A11}$$

We also have the relation $V(r)=V_e(r)+V_n(r)$. Using these relations, $E_{\rm pot}$ can be expressed as

$$E_{\rm pot}=-\tfrac{1}{2}4\pi e\int_0^{r_0}r^2dr\,n(r)\left[V(r)+\frac{Ze}{r}\right], \tag{A12}$$

or, in terms of the new notation

$$\begin{aligned}E_{\rm pot}=&-\frac{aZkT}{\Psi(0)}\int_0^1 dx\,xJ_{1/2}\left[\frac{\Psi(x)}{x},\Psi(1)\right]\\&\times[\Psi(x)-\Psi'(1)x+\Psi(0)]\\=&\frac{ZkT}{\Psi(0)}\left[-\Psi(1)\Psi'(1)+\Psi(0)\Psi'(0)-[\Psi'(1)]^2\right.\\&\left.-\tfrac{1}{2}\int_0^1 dx[\Psi'(x)]^2\right].\end{aligned} \tag{A13}$$

From Eqs. (A5) and (A13), then, it follows that

$$2E_{\rm kin}+E_{\rm pot}=0\ . \tag{A14}$$

The pressure, expressed as the rate of transfer of momentum between the electrons and the ion boundary, is given by

$$P=\frac{8\pi^2}{h^3}\int_0^{p_m}\frac{p^2(p^2/3m)}{\exp[(p^2/2m-\alpha)/kT]+1}dp\ . \tag{A15}$$

From the definition of p_m in Eq. (4), we notice that at the ion boundary p_m in Eq. (A15) vanishes, resulting in zero pressure at the boundary. Therefore the derivation of Eq. (A14) is actually a verification of the virial theorem.

Note that the validity of the virial theorem is well known in the customary TF model. Now, in spite of the

fact that in our model the bound electrons are defined by a momentum cutoff integral, the virial theorem is still proven to hold true.

APPENDIX B: DERIVATION OF THE FREE ENERGY OF THE BOUND ELECTRONS

In the noninteracting Fermi system, if n_i is the mean occupation number of electrons in the ith quantum state, the entropy of the system can be derived from first principles as

$$S=-k\sum_i [n_i \ln n_i+(1-n_i)\ln(1-n_i)] , \tag{B1}$$

where the summation of i should be over all the quantum states available. The distribution n_i is the Fermi-Dirac distribution function

$$n_i=\frac{1}{\exp[(\varepsilon_i-\alpha)/kT]+1} , \tag{B2}$$

where ε_i is the energy of an electron in ith quantum state and α is a constant whose value is determined by the normalization condition

$$\sum_i \frac{1}{\exp[(\varepsilon_i-\alpha)/kT]+1}=N , \tag{B3}$$

where N is the total number of particles in the system.

From Eqs. (B1) and (B2) the entropy of the bound-electron system within the ion may be written as

$$\begin{aligned} TS&=\sum_i [n_i(\varepsilon_i-\alpha)-kT\ln(1-n_i)] \\ &=\sum_i [n_i(\varepsilon_{\mathrm{kin},i}+\varepsilon_{e\text{-}n,i}+\varepsilon_{e\text{-}e,i}-\alpha) \\ &\quad -kT\ln(1-n_i)] , \end{aligned} \tag{B4}$$

where $\varepsilon_{\mathrm{kin},i}$, $\varepsilon_{e\text{-}e,i}$ are the kinetic energy of the electron in the ith state, the potential energy between the electron in the ith state and the nucleus, and the potential energy between the electron in the ith state and the other electrons within the ion, respectively.

The total energy of the bound electrons is given by

$$E=\sum_i [n_i(\varepsilon_{\mathrm{kin},i}+\varepsilon_{e\text{-}n}+\tfrac{1}{2}\epsilon_{e\text{-}i})] . \tag{B5}$$

The total electron-electron potential energy per atom is given by

$$E_{e\text{-}e}=\tfrac{1}{2}\sum_i n_i\varepsilon_{e\text{-}e,i} . \tag{B6}$$

In terms of Eqs. (B5) and (B6), Eq. (B4) may be rewritten as

$$TS=E+E_{e\text{-}e}-(Z-z)\alpha-kT\sum_i \ln(1-n_i) , \tag{B7}$$

where $Z-z$ is the total number of bound electrons within the ion. Therefore the free energy of the bound electrons is

$$F_1=E-TS=(Z-z)\alpha-E_{e\text{-}e}+kT\sum_i \ln(1-n_i) . \tag{B8}$$

The last term in Eq. (B8) can be calculated as follows:

$$\begin{aligned} kT\sum_i \ln(1-n_i)&=-\frac{32\pi^2kT}{h^3}\int_0^{r_0} dr\, r^2\int_0^{p_m} dp\, p^2 \ln\left[1+\exp\left[\frac{\alpha+eV(r)-p^2/2m}{kT}\right]\right] \\ &=-\frac{aZkT}{\Psi(0)}\int_0^1 dx\, x^2\int_0^{\Psi(x)/x-\Psi(1)} dy\, y^{1/2}\ln\left[1+\exp\left[\frac{\Psi(x)}{x}-y\right]\right] \\ &=-\frac{2}{3}\frac{aZkT}{\Psi(0)}\int_0^1 dx\, x^2\left\{y^{3/2}\ln\left[1+\exp\left[\frac{\Psi(x)}{x}-y\right]\right]\right\}\Bigg|_0^{\Psi(x)/x-\Psi(1)} \\ &\quad -\frac{2}{3}\frac{aZkT}{\Psi(0)}\int_0^1 dx\, x^2\int_0^{\Psi(x)/x-\Psi(1)} dy\, y^{3/2}\frac{\exp[\Psi(x)/x-y]}{\exp[\Psi(x)/x-y]+1} \\ &=-\frac{2}{3}\frac{aZkT}{\Psi(0)}\ln(1+\exp[\Psi(1)])\int_0^1 dx\, x^2\left[\frac{\Psi(x)}{x}-\Psi(1)\right]^{3/2} \\ &\quad -\frac{2}{3}\frac{aZkT}{\Psi(0)}\int_0^1 dx\, x^2 J_{3/2}\left[\frac{\Psi(x)}{x},\Psi(1)\right] \\ &=-\frac{2}{3}\frac{aZkT}{\Psi(0)}\ln(1+\exp[\Psi(1)])\int_0^1 dx\, x^2\left[\frac{\Psi(x)}{x}-\Psi(1)\right]^{3/2}-\tfrac{2}{3}E_{\mathrm{kin}} \\ &=-\frac{2}{3}\frac{aZkT}{\Psi(0)}\ln(1+\exp[\Psi(1)])\int_0^1 dx\, x^2\left[\frac{\Psi(x)}{x}-\Psi(1)\right]^{3/2}-\tfrac{1}{3}E_{\mathrm{pot}} . \end{aligned} \tag{B9}$$

In the last step, the virial theorem expressed by Eq. (A14) has been applied. Substituting Eq. (B9) for the last term in Eq. (B8) and employing the expressions for $E_{\rm pot}$ in Eq. (A12) and $E_{e\text{-}e}$ in Eq. (A7) lead to the expression given for F_1 in Eq. (14).

APPENDIX C: EXPRESSION OF THE CHEMICAL POTENTIAL OF BOUND ELECTRONS

An explicit expression for the chemical potential of the bound electrons can be derived from the free energy of the bound electrons through the relation

$$\mu_1=\frac{\partial F_1}{\partial(Z-z)}\bigg|_{r_0} . \tag{C1}$$

The derivation starts from Eq. (B8), which gives

$$F_1=E-TS=(Z-z)\alpha-E_{e\text{-}e}+kT\sum_i \ln(1-n_i) . \tag{C2}$$

By combining Eqs. (A7) and (A9), the second term in Eq. (C2) can be written as

$$E_{e\text{-}e}=\tfrac{1}{2}(4\pi e)^2\int_0^{r_0} r^2dr\int_0^{r_0} r'^2dr'\frac{n(r)n(r')}{|\mathbf{r}-\mathbf{r}'|} , \tag{C3}$$

which leads to

$$\frac{\partial E_{e\text{-}e}}{\partial z}=(4\pi e)^2\int_0^{r_0} r^2dr\int_0^{r_0} r'^2dr'\frac{n(r)}{|\mathbf{r}-\mathbf{r}'|}\frac{\partial n(r')}{\partial z} . \tag{C4}$$

The third term in Eq. (C2) can be written as

$$kT\sum_i \ln(1-n_i)=-\frac{32\pi^2kT}{h^3}\int_0^{r_0} dr\,r^2\int_0^{p_m} dp\,p^2\ln\left[1+\exp\left[\frac{\alpha+eV(r)-p^2/2m}{kT}\right]\right] . \tag{C5}$$

Noting that $p_m=\{2me[V(r)-V_0]\}^{1/2}$ is also a function of z, the derivative of Eq. (C5) with respect to z turns out to be

$$kT\frac{\partial}{\partial z}\sum_i \ln(1-n_i)=-4\pi\int_0^{r_0} dr\,r^2n(r)\left[\frac{\partial eV(r)}{\partial z}+\frac{\partial\alpha}{\partial z}\right]$$
$$-\frac{32\pi^2kT}{h^3}\ln\left[1+\exp\left[\frac{\alpha+eV_0}{kT}\right]\right]\frac{1}{3}(2me)^{3/2}\frac{\partial}{\partial z}\int_0^{r_0} dr\,r^2[V(r)-V_0]^{3/2} , \tag{C6}$$

where Eq. (A11) has been used.

From the relation $V(r)=V_e(r)+V_n(r)$, Eqs. (A9) and (A10), we have

$$V(r)=\frac{Ze}{r}-4\pi e\int_0^{r_0} r'^2dr'\frac{n(r')}{|\mathbf{r}-\mathbf{r}'|} . \tag{C7}$$

Substituting Eq. (C7) into Eq. (C6) leads to

$$kT\frac{\partial}{\partial z}\sum_i \ln(1-n_i)=(4\pi e)^2\int_0^{r_0} dr\,r^2\int_0^{r_0} dr'r'^2\frac{n(r')}{|\mathbf{r}-\mathbf{r}'|}\frac{\partial n(r')}{\partial z}-(Z-z)\frac{\partial\alpha}{\partial z}$$
$$-\frac{32\pi^2kT}{3h^3}\ln\left[1+\exp\left[\frac{\alpha+eV_0}{kT}\right]\right](2me)^{3/2}\frac{\partial}{\partial z}\int_0^{r_0} dr\,r^2[V(r)-V_0]^{3/2} . \tag{C8}$$

From Eqs. (C2), (C3), and (C8), one finally finds

$$\mu_1=\frac{\partial F_1}{\partial(Z-z)}$$
$$=\alpha+\frac{32\pi^2kT}{3h^3}\ln\left[1+\exp\left[\frac{\alpha+eV_0}{kT}\right]\right](2me)^{3/2}$$
$$\times\frac{\partial}{\partial z}\int_0^{r_0} dr\,r^2[V(r)-V_0]^{3/2} . \tag{C9}$$

Obviously the chemical potential μ_1 is not identical to the constant α.

APPENDIX D: DETERMINATION OF THE FREE ENERGY IN THE SECOND APPROXIMATION

The energy of the test ion is

$$E=E_0+E_I+E_{i\text{-}i} , \tag{D1}$$

where E_0 is the translational kinetic energy of the test ion (including the nucleus and the electrons), E_I is the internal energy of the test ion, and $E_{i\text{-}i}$ is the ion-ion correlation energy from the interaction of this test ion with the neighboring ions, which are regarded as point charges.

The term E_I in Eq. (D1) is given by

$$E_I=E_{{\rm kin},b}+E_{b\text{-}n}+E_{b\text{-}b} , \tag{D2}$$

where $E_{{\rm kin},b}$ is the kinetic energy of the bound electrons related to the internal motion, $E_{b\text{-}n}$ is the bound-electron–nucleus interaction energy within the ion, and $E_{b\text{-}b}$ is the bound-electron–bound-electron interaction energy within the ion.

The terms in Eq. (D2) are given as follows:

$$E_{\mathrm{kin},b}=\frac{32\pi^2}{h^3}\int_0^{r_0} r^2dr\int_0^{p_m}\frac{p^2(p^2/2m)}{\exp\{[p^2/2m-eV(r)-\alpha]/kT\}+1}dp\ , \tag{D3}$$

$$E_{b\text{-}n}=-4\pi Ze^2\int_0^{r_0} r\,dr\,n_b(r)\ , \tag{D4}$$

and

$$E_{b\text{-}b}=-\tfrac{1}{2}4\pi e\int_0^{r_0} r^2dr\,n_b(r)V_b(r)\ , \tag{D5}$$

with

$$V_b(r)=-4\pi e\int_0^{r_0} r'^2dr'\frac{n_b(r')}{|\mathbf{r}-\mathbf{r}'|}\ , \tag{D6}$$

and

$$n_b(r)=\frac{8\pi}{h^3}\int_0^{p_m}\frac{p^2}{\exp\{[p^2/2m-eV(r)-\alpha]/kT\}+1}dp\ . \tag{D7}$$

The derivation of the term $E_{i\text{-}i}$ in Eq. (D1) is as follows.

Singling out a test ion, the interaction energy between the bound electrons in this test ion and the neighboring ions (with a neutral background, i.e., including the free electrons) is given by

$$E^*_{b\text{-}i}=-4\pi e\int_0^{r_0} r^2dr\,n_b(r)V_i(r)\ , \tag{D8}$$

and the interaction energy between the nucleus of this test ion and the neighboring ions (with a neutral background) is given by

$$E^*_{n\text{-}i}=ZV_i(0)\ , \tag{D9}$$

with

$$V_i(r)=-4\pi ze\int_0^{\infty} r'^2dr'e\frac{g_i(r')}{|\mathbf{r}-\mathbf{r}'|} \tag{D10}$$

and

$$g_i(r)=n_i\left[\exp\left[-\frac{zeV(r)}{kT}\right]-1\right]\ . \tag{D11}$$

Note that here the neighboring ions are treated as point charges.

Now, considering the entire system of N ions, the total contribution to the energy from the ion-ion correlation effect is

$$E_{\mathrm{cor}}=\tfrac{1}{2}N(E^*_{b\text{-}i}+E^*_{n\text{-}i})\ , \tag{D12}$$

where the $\frac{1}{2}$ factor is needed to avoid double counting and $E_{i\text{-}i}$ in Eq. (D1), which is ion-ion correlation energy per ion, is given by

$$E_{i\text{-}i}=\frac{E_{\mathrm{corr}}}{N}=\tfrac{1}{2}E^*_{b\text{-}i}+\tfrac{1}{2}E^*_{n\text{-}i}\ . \tag{D13}$$

Introducing $E_{b\text{-}i}=\frac{1}{2}E^*_{b\text{-}i}$ and $E_{n\text{-}i}=\frac{1}{2}E^*_{n\text{-}i}$ as the bound-electron–neighboring-ion and nucleus–neighboring-ion interaction energies averagely shared by each ion, we have

$$E_{i\text{-}i}=E_{b\text{-}i}+E_{n\text{-}i}\ . \tag{D14}$$

Turning now to the entropy of the test ion, we can split the entropy similarly to the energy in Eq. (D1),

$$S=S_0+S_I+S_{i\text{-}i}\ , \tag{D15}$$

where S_0 is the entropy related to the translational motion of the ion, S_I is the entropy related to the internal motion within the ion, and $S_{i\text{-}i}$ is the entropy contributed by the ion-ion correlation effect.

The term S_I in Eq. (D15) can be derived in the same manner as in Appendix B and is given by

$$\begin{aligned}TS_I=\sum_i\left[n_i(\varepsilon_i-\alpha)-kT\sum_i\ln(1-n_i)\right]&=E_{\mathrm{kin},b}+E_{b\text{-}n}+2E_{b\text{-}b}+2E_{b\text{-}i}+(Z-z)\alpha-kT\sum_i\ln(1-n_i)\\&=E_I+E_{b\text{-}b}+2E_{b\text{-}i}+(Z-z)\alpha-kT\sum_i\ln(1-n_i)\ .\end{aligned} \tag{D16}$$

The free energy of the test ion is

$$F=F_0+F_I+F_{i\text{-}i}\ , \tag{D17}$$

where F_0 is the free energy related to the translational motion of the ion, F_I is the free energy related to the internal motion within the ion given by

$$F_I=F_I-TS_I\ , \tag{D18}$$

and $F_{i\text{-}i}$ is the free energy contributed by the ion-ion correlation effect.

The free energy of the combined ion and free-electron system is

$$\begin{aligned}F_{\mathrm{tot}}=F+F_{\mathrm{free}}&=F_0+F_I+F_{i\text{-}i}+F_{\mathrm{free}}\\&=F_0-E_{b\text{-}b}-2E_{b\text{-}i}+(Z-z)\alpha-kT\sum_i\ln(1-n_i)+F_{i\text{-}i}+F_{\mathrm{free}}\\&=F_0-(E_{b\text{-}b}+E_{b\text{-}i})+(Z-z)\alpha-kT\sum_i\ln(1-n_i)+F_{i\text{-}i}-E_{b\text{-}i}+F_{\mathrm{free}}\ ,\end{aligned} \tag{D19}$$

where the F_{free} is the free energy of the free electrons. The term F_0 only depends on the temperature and ion density, and therefore is irrelevant to the minimization of F_{tot}.

From Eqs. (D5) and (D8) the term $E_{b\text{-}i}+E_{b\text{-}b}$ in Eq. (D19) can be calculated by the following formula:

$$E_{b\text{-}i}+E_{b\text{-}b}=-\tfrac{1}{2}4\pi e\int_0^{r_0} r^2dr\, n_b(r)[V_b(r)+V_i(r)]=-2\pi e\int_0^{r_0} r^2dr\, n_b(r)\left[V(r)-\frac{Ze}{r}\right], \tag{D20}$$

and the term $kT\sum_i \ln(1-n_i)$ is calculated as

$$kT\sum_i \ln(1-n_i)=-\frac{32\pi^2}{h^3}kT\int_0^{r_0} r^2dr\int_0^{p_m} p^2dp\ln\left[\exp\left[\frac{p^2/2m-eV(r)-\alpha}{kT}\right]+1\right]. \tag{D21}$$

F_{free} is given by Eq. (15) or (16).

Although the term $E_{b\text{-}i}+E_{b\text{-}b}$ can be calculated through Eq. (D20), the term $E_{b\text{-}i}$ alone must be calculated through Eq. (D8), which involves a double integration. An exact calculation of the term $F_{i\text{-}i}$ should be done through an integration of $E_{i\text{-}i}$, which from Eq. (D14) consists of the term $E_{b\text{-}i}$ as well. An excessively large amount of computer time, however, is required to carry out the double integration involved in the calculation of $E_{b\text{-}i}$. To make this calculation tractable, the terms $F_{i\text{-}i}$ and $E_{b\text{-}i}$ have been approximated by the results from the nonlinear Debye-Hückel theory.[50] Actually, this approximation simply means that concerning the calculation of the ion-ion correlation energy and free energy, the central ion is treated as a point charge without inner structure.

Thus $E_{b\text{-}i}$ can be expressed as

$$E_{b\text{-}i}=\frac{(z-1)E_{i\text{-}i}}{z}, \tag{D22}$$

where $E_{i\text{-}i}$ is the average correlation energy between ions of charge ze for each ion. In the nonlinear Debye-Hückel theory,[50] $E_{i\text{-}i}/kT$ is given as a function of the plasma parameter $\Gamma=z^2e^2/(r_0kT)$ only.

The term $F_{i\text{-}i}/kT$, which is also a function of Γ only, is derived from the formula

$$\frac{F_{i\text{-}i}(\Gamma)}{kT}=\int_0^{\Gamma}\frac{d\Gamma'}{\Gamma'}\frac{E_{i\text{-}i}(\Gamma')}{kT}. \tag{D23}$$

Practically, the integration in Eq. (D23) starts from some small Γ ($\Gamma=0.001$) by adopting the linear DH results given by an analytic formula

$$\frac{F_{i\text{-}i}(\Gamma)}{kT}=-\frac{\Gamma^{3/2}}{\sqrt{3}} \tag{D24}$$

as the initial value.

*Present address: Department of Chemical Engineering, Florida State University, Tallahassee, FL 32316-2175.

[1]A. N. Cox, in *Stellar Structure,* edited by L. H. Aller and D. B. McLaughli (University of Chicago Press, Chicago, 1965).
[2]W. Ebeling, W. D. Kraeft, and D. Kremp, *Theory of Bound States and Ionization Equilibrium in Plasmas and Solids* (Academie-Verlag, Berlin, 1976).
[3]W. D. Kraeft, D. Kemp, W. Ebeling, and G. Ropke, *Quantum Statistics of Charged Particle System* (Academie-Verlag, Berlin, 1986).
[4]G. Kalman, R. Ying, and R. Hogaboom, in Proceedings of the International Conference on Plasma Science, San Diego, 1983 (unpublished).
[5]S. Kobayashi, J. Phys. Soc. Jpn. **14**, 1039 (1959).
[6]R. Latter, Phys. Rev. **99**, 1854 (1955).
[7]R. Latter, J. Chem. Phys. **26**, 270 (1956).
[8]R. Feynman, N. Metropolis, and E. Teller, Phys. Rev. **75**, 1561 (1949).
[9]W. Ebeling, Physica **38**, 378 (1968).
[10]W. Zimdahl and W. Ebeling, Ann. Phys. (Leipzig) **34**, 9 (1977).
[11]W. Ebeling, C. V. Meister, and R. Sandig, Ann. Phys. (Leipzig) **36**, 321 (1979).
[12]H. Dienemann, G. Clemens, and W. D. Kraeft, Ann. Phys. (Leipzig) **37**, 444 (1980).
[13]D. Kremp, W. D. Kraeft, and A. J. D. Lambert, Physica **127A**, 72 (1984).
[14]W. Ebeling, A. Forster, and W. Richert, Physica A **150**, 159 (1988).
[15]W. Ebeling, A. Forster, R. Redmer, T. Rother, and M. Schlanges, in *Proceedings of the XVIII Conference on Phenomena in Ionized Gases,* edited by W. T. Williams (Hilger, Bristol, 1987).
[16]F. J. Rogers, H. C. Graboske, Jr., and D. J. Harwood, Phys Rev. A **1**, 1577 (1970).
[17]F. J. Rogers, H. C. Graboske, Jr., and H. E. DeWitt, Phys. Lett **34A**, 127 (1971).
[18]F. J. Rogers, Phys. Lett. **61A**, 358 (1977).
[19]F. J. Rogers, Astrophys. J. **310**, 723 (1986).
[20]R. M. More, in *Applied Atomic Collision Physics,* edited by H. S. Massey (Academic, New York, 1983), Vol. II.
[21]P. Hohenberg and W. Kohn, Phys. Rev. **136**, B864 (1964).
[22]M. W. C. Dharma-wardana and F. Perrot, Phys. Rev. A **26**, 2096 (1982); M. W. C. Dharma-wardana, in *Strongly Coupled Plasma Physics,* edited by F. J. Rogers and H. E. DeWitt (Plenum, New York, 1987).
[23]F. Perrot, in Ref. 22, p. 293.
[24]J. C. Stewart and K. D. Pyatt, Jr., Astrophys. J. **144**, 1203 (1966).
[25]J. C. Weisheit and B. F. Rozsnyai, J. Phys. B **9**, L63 (1976).
[26]B. F. Rozsnyai, Phys. Rev. A **5**, 1137 (1972).
[27]S. Skupsky, Phys. Rev. A **21**, 1316 (1980).
[28]J. Davis and M. Blaha, in *Physics of Electronic and Atomic Collisions,* edited by S. Datz (North-Holland, New York, 1982).

[29]R. Cauble, M. Blaha, and J. Davis, Phys. Rev. A **29**, 3280 (1984).
[30]G. A. Rinker, Phys. Rev. A **37**, 1284 (1988).
[31]G. A. Rinker, Phys. Rev. B **31**, 4207 (1985); **31**, 4220 (1985).
[32]R. D. Cowan and J. G. Kirkwood, J. Chem. Phys. **29**, 264 (1958).
[33]B. F. Rozsnyai and B. J. Alder, Phys. Rev. A **14**, 2295 (1976).
[34]R. F. Rozsnyai, Phys. Rev. A **16**, 1687 (1977).
[35]R. More, Phys. Rev. A **19**, 1234 (1979).
[36]I. J. Feng, W. Zakowicz, and R. H. Pratt, Phys. Rev. A **23**, 883 (1981).
[37]W. Zakowicz, I. J. Feng, and R. H. Pratt, J. Quant. Spectrosc. Radiat. Transfer **27**, 329 (1982).
[38]A preliminary report on this work has been given by R. Ying and G. Kalman, in Ref. 22, p. 267 and R. Ying and G. Kalman, in Proceedings of the XVIII International Conference on Phenomena in Ionized Gases, Swansea, Great Britain, 1987 (unpublished).
[39]K. C. Ng, J. Chem. Phys. **61**, 2680 (1974).
[40]D. D. Carley, Phys. Rev. **131**, 1406 (1963).
[41]J. F. Springer, M. A. Pokrant, and F. A. Stevens Jr., J. Chem. Phys. **58**, 4863 (1973).
[42]F. J. Rogers, D. A. Young, H. E. DeWitt, and M. Ross, Phys. Rev. A **28**, 2990 (1983).
[43]K. S. Singwi, M. P. Tosi, R. H. Land, and A. Sjolander, Phys. Rev. **176**, 589 (1968).
[44]K. S. Singwi, A. Sjolander, M. P. Tosi, and R. H. Land, Solid State Commun. **7**, 1503 (1969).
[45]K. S. Singwi, A. Sjolander, M. P. Tosi, and R. H. Land, Phys. Rev. B **1**, 1044 (1970).
[46]Y. Rosenfeld and N. W. Ashcroft, Phys. Rev. A **20**, 1208 (1979).
[47]Y. Rosenfeld, Phys. Rev. Lett. **44**, 146 (1980).
[48]Y. Rosenfeld, J. Stat. Phys. **37**, 215 (1984).
[49]See, e.g., R. L. Shepherd, D. R. Kania, and L. A. Jones, Phys. Rev. Lett. **61**, 1278 (1989); **61**, 2900(E) (1989).
[50]J. T. Hansen, Phys. Rev. A **8**, 3096 (1973).